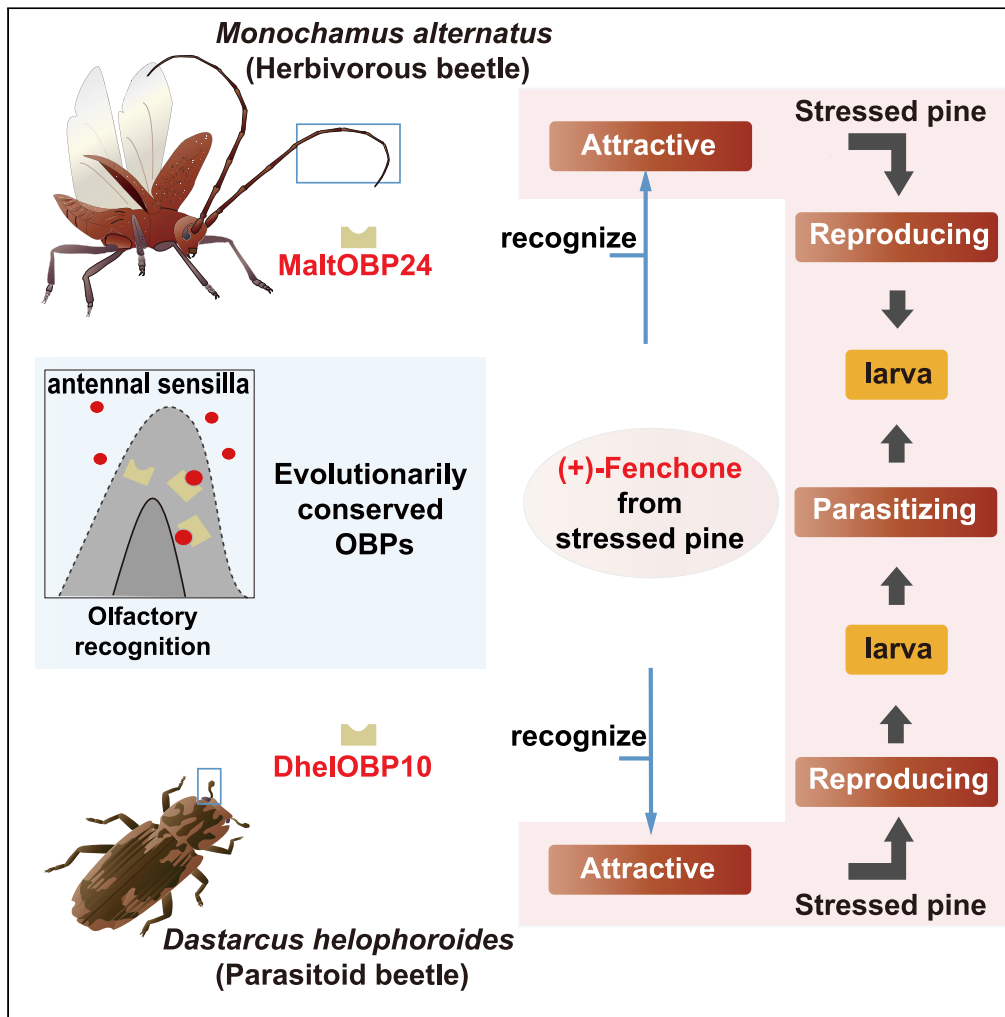**Article**

Evolutionarily conserved odorant-binding proteins participate in establishing tritrophic interactions

Ruinan Yang,
Dongzhen Li,
Shancheng Yi,
Manqun Wang

mqwang@mail.hzau.edu.cn

Highlights

Monochamus alternatus and *Dastarcus helophoroides* are attracted to (+)-fenchone from host pines

They harbor evolutionarily conserved odorant-binding proteins (OBPs)

One pair of the conserved OBPs can bind with (+)-fenchone

The behavioral preference is lost upon RNAi knockdown of the OBPs

Article

Evolutionarily conserved odorant-binding proteins participate in establishing tritrophic interactions

Ruinan Yang,[1] Dongzhen Li,[1,2] Shancheng Yi,[1] and Manqun Wang[1,3,*]

SUMMARY

Attracting herbivores and their natural enemies is a standard method where plant volatiles mediate tritrophic interactions. However, it remains unknown whether the shared attraction has a shared chemosensory basis. Here we focus on the odorant-binding proteins (OBPs), a gene family integral to peripheral detection of odoriferous chemicals. Previous evidence suggests that the herbivorous beetle *Monochamus alternatus* and its parasitoid beetle *Dastarcus helophoroides* are attracted to stressed pines. In this study, (+)-fenchone, emitted by stressed pines, is found to be attracted to *M. alternatus* and *D. helophoroides* in behavioral assays. Meanwhile, two orthologous OBPs with a slower evolutionary rate, respectively, from the two insects are shown to bind with (+)-fenchone, and the attraction is abolished after RNAi. These results show the ability of evolutionarily conserved OBPs from herbivores and their enemies to detect the same plant volatiles, providing an olfactory mechanism of chemical signals–mediated tritrophic relationships.

INTRODUCTION

Tritrophic interactions among host plants, herbivores, and their natural enemies are essential to terrestrial ecosystems (Price et al., 1980; Turlings and Erb, 2018). Plant volatiles have received considerable critical attention as searching cues for herbivorous insects to locate host plants and for natural enemies, such as predators and parasitoids, to find prey or hosts (Aartsma et al., 2017; Bruce et al., 2005; Li et al., 2015). Insects have evolved sensitive and specific olfactory perception mechanisms to perceive this information (Ache and Young, 2005; Hansson and Stensmyr, 2011). Odoriferous chemicals released by plants, which generally are hydrophobic molecules, penetrate through the cuticle pores at the surface of antennal sensilla, bind with odorant-binding proteins (OBPs) specifically, and are transported through the hydrophilic sensillar lymph to olfactory receptor neurons (ORNs). Olfactory receptors (ORs) located at the membrane of ORNs identify these molecules and trigger olfactory nerve impulses that elicit behavioral responses (Brito et al., 2016; Hansson, 2002; Leal, 2013).

Evolutionary conservation and differentiation of OBP genes is one of the foundations of olfactory perception, including binding and recognizing odors selectively and regulating different behavioral choices. As a link between the environment and individual behavioral responses, their evolution is strongly associated with ecological adaptions (Swarup et al., 2011; Vandermoten et al., 2011; Vieira and Rozas, 2011; Wang et al., 2019). On the one hand, the high divergency of OBP genes provides a molecular basis and possibility for functional diversity. For instance, the larger OBP gene repertoire in the pea aphid *Acyrthosiphon pisum* may be related to its broader host range versus the specialization of soybean aphids *Aphis glycines* on a single summer host plant (Robertson et al., 2019). In addition, the evolutionary conservation of OBPs is related with functional similarity. Evolutionarily conserved OBPs are common in closely related species of herbivores from the same order or lower grades. Conserved pheromone-binding proteins (PBPs), a subfamily of OBPs, from many species of moths share the ability to detect sex pheromones (Gu et al., 2013; Jing et al., 2020; Maida et al., 2003; Vogt and Riddiford, 1981). SfurOBP11, NlugOBP8, and LstrOBP2, respectively, from the three rice planthoppers *Sogatella furcifera*, *Nilaparvata lugens*, and *Laodelphax striatellus*, are essential for complete ability to locate rice plants. They show a slower evolution rate and are more conserved (He et al., 2019). These species usually have broadly overlapping host plant ranges or have the same or similar pheromone components. They may use the conserved OBPs through evolution to detect these plant volatiles or pheromones as chemical cues to avoid resource competition with other species, or to locate hosts (Farias et al., 2015).

[1]Hubei Insect Resources Utilization and Sustainable Pest Management Key Laboratory, College of Plant Science and Technology, Huazhong Agricultural University, Wuhan 430070, China

[2]Key Laboratory of Forest Protection of National Forestry and Grassland Administration, Ecology and Nature Conservation Institute, Chinese Academy of Forestry, Beijing 100091, China

[3]Lead contact

*Correspondence:
mqwang@mail.hzau.edu.cn
https://doi.org/10.1016/j.isci.2022.104664

Evolutionarily conserved OBPs also exist in herbivores and their natural enemies. SaveOBP3 in the grain aphid *Sitobion avenae* and two OBPs of its predators, EbalOBP3 in the marmalade hoverfly *Episyrphus balteatus* and HaxyOBP3 in the multicolored Asian lady beetle *Harmonia axyridis* are in the same cluster with amino acid sequence similarities more than 90%. Both SaveOBP3 and EbalOBP3 are found to have high affinity with the alarm pheromone (E)-β-farnesene in fluorescence-binding assays, but their olfactory function has not been affirmed (Beale et al., 2006; Du et al., 1998; Vandermoten et al., 2011).

Fruitful comparative analyses of evolutionarily conserved OBPs from herbivores and natural enemies are always difficult. Few evolutionarily conserved OBPs from herbivores and their natural enemies reported sharing a high sequence similarity and specific binding capacity like SaveOBP3 and EbalOBP3, especially when these OBPs are from different orders. Furthermore, OBPs show relative broad binding affinities and a varying degree of binding specificity, especially when they bind with plant volatiles (Carey et al., 2010; Dani et al., 2010; de Fouchier et al., 2017; Li et al., 2018). Therefore, more shreds of evidence are needed to show how these OBPs participate in ecological adaptations.

Here, we described a tritrophic interaction model combining pine trees, Japanese sawyer beetle *Monochamus alternatus* Hope (Coleoptera: Cerambycidae), and its parasitoid beetle *Dastarcus helophoroides* Fairmaire (Coleoptera: Bothrideridae). *M. alternatus* is a severe pest in several pine and fir species (Kobayashi et al., 1984). Sexually matured adults of *M. alternatus* seek diseased and dying pine trees as the spawning place (Hanks, 1999). *D. helophoroides* is a prominent natural enemy of *M. alternatus*, which spawns near the tunnels and pupal chambers of *M. alternatus* larva, and parasitizes the larva and pupa after hatching(Wei et al., 2009; Yang et al., 2014). In this study, one monoterpenoid volatile, (+)-fenchone, from stressed pine trees is found to have the potential to act as one of the vital chemical clues that guide *M. alternatus* from feeding fresh trees to stressed trees for mating and ovipositing and lead *D. helophoroides* to locate the habitat of *M. alternatus* for parasitism (Hanks, 1999; Mi and Wang, 2020; Wei et al., 2009). Moreover, we identify a pair of evolutionarily conserved OBPs, MaltOBP24 from *M. alternatus* and DhelOBP10 from *D. helophoroides*, which play an essential role in detecting (+)-fenchone. By testing multiple tritrophic systems throughout the insects, we find that although OBPs are generally highly divergent, several cases of OBP orthologs under purifying selection with elevated sequence similarity and similar motif structure exist between the common herbivores and their enemies, suggesting they are more conserved and might share a similar chemosensory function. This research depicts a scene of a chemical signal-mediated pine–longicorn–enemy interaction and indicates an olfactory molecular mechanism under it by demonstrating that evolutionarily conserved OBPs can function similarly in detecting volatiles from the host plant.

RESULTS

Behavior choice of *M. alternatus* and *D. helophoroides* adults to (+)-fenchone

Typical tritrophic interactions exist in Pine trees, Japanese sawyer beetle *M. alternatus* Hope and *D. helophoroides*. Here, through a Y-tube experiment, we confirmed that *M. alternatus* and *D. helophoroides* adults were significantly attracted by (+)-fenchone, which indicated (+)-fenchone may be one of the important chemical signals that mediate this tritrophic interaction (Figure 1). In this model, our research focuses on whether some evolutionarily conserved OBPs are participating in recognizing (+)-fenchone and establishing tritrophic interactions.

Screening functional OBPs by phylogenetic analysis

Phylogenetic analysis was performed using amino acid sequences of 223 OBPs from 10 species of eight superfamilies in Coleoptera, including *M. alternatus* (Chrysomeloidea), *D. helophoroides* (Coccinelloidea), *H. axyridis* (Coccinelloidea), *Colaphellus bowringi* (Chrysomeloidea), *Cylas formicarius* (Curculionoidea), *Aethina tumida* (Cucujoidea), *Tribolium castaneum* (Tenebrionoidea), *Rhyzopertha dominica* (Bostrichoidea), *Holotrichia oblita* (Scarabaeoidea), and *Nicrophorus vespilloides* (Staphylinoidea). The results revealed that there were four pairs of OBPs respectively belonging to *M. alternatus* and *D. helophoroides* in the same clusters with high bootstrap support (≥70) (Figure 2). Each pair defined a unique clade with homologous members from different coleopteran superfamilies. Selection pressure analyses indicated that each clade may evolve under strong purifying selection with ω < 1 (ω = dN/dS) (Table 1), which is consistent with previous studies on insect OBP evolution (He et al., 2019; Vieira et al., 2007). Pairwise comparisons of site models (both M1a-M2a and M7- M8) by the likelihood ratio test (LRT) also suggested purifying selection for Clades A, B, and C. As for Clade D, the more stringent comparison, M1a-M2a
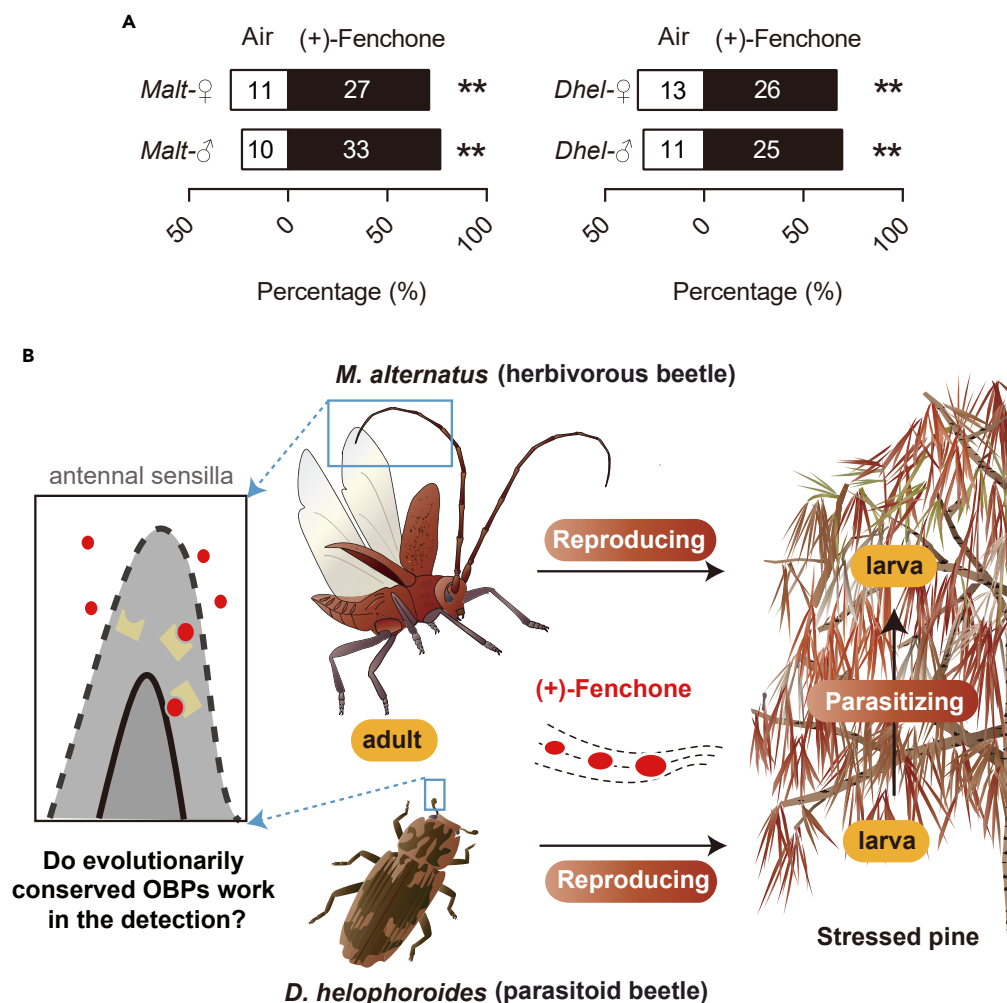
Figure 1. (+)-Fenchone mediating tritrophic interactions among pine trees, *M. alternatus* and *D. helophoroides*

(A) Behavioral responses of 8-day *M. alternatus* adults and unmated *D. helophoroides* adults to (+)-fenchone. Selectivity represented the percentage of beetles with credible behavior choices. The number in the column indicated the total number of beetles choosing the arm. "**" indicated $p < 0.01$. p-values were determined by the Chi-square test.

(B) A tritrophic interaction model combined with pine trees, *M. alternatus* and *D. helophoroides*. (+)-Fenchone, a volatile from stressed pine trees, can be detected by matured *M. alternatus* adults and *D. helophoroides* adults via an olfactory system including odorant-binding proteins. It may act as a vital chemical clue that guides *M. alternatus* from feeding fresh trees to stressed trees for mating and ovipositing and leads *D. helophoroides* to locate *M. alternatus* for parasite in the long-distance range.

implied purifying selection, whereas M7 vs M8 showed that positive selection models are significantly more likely (Table 1).

The rate of molecular evolution k_{aa} was then analyzed to provide more specific amino acid sequence information of the four pairs of OBPs. Owing to the same T value (the number of years that *M. alternatus* and *D. helophoroides* have elapsed since divergence from a common ancestor), k_{aa} depends only on K_{aa}. Therefore, MaltOBP24 and DhelOBP10 have evolved with the slowest evolution rate among the four pairs of OBPs (Table 2). Along with their relatively high amino acid identity (50%) and similarity (68.1%) (Table 2, Figure S1A), we decided to delve into their functional properties involved in interspecific interaction.

Comparative analyses based on the sequences indicated many similarities in physicochemical properties, including the length of the open reading frame, molecular weight, the length of signal peptides, and isoelectric points (Table S1). Based on the conserved cysteine patterns in their sequences, insect OBPs are
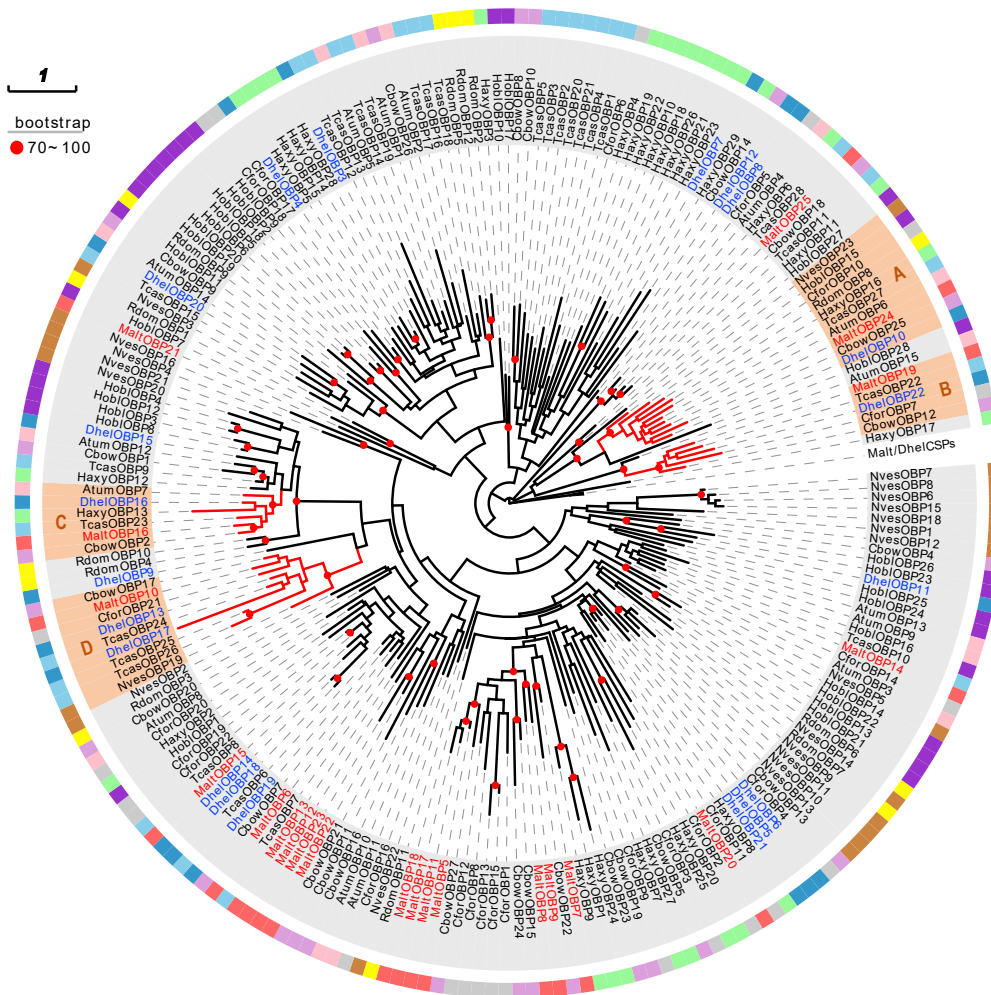
Figure 2. Phylogenetic analysis of OBPs in Coleoptera

The amino acid sequences (without signal peptides) of 223 OBPs from 10 species of eight superfamilies in Coleoptera based on the maximum likelihood algorithm. Bootstrap values larger than 70 are labeled with red dots on the nodes. The protein names and sequences used in this analysis are listed in Table S4. Malt, *M. alternatus* (Chrysomeloidea); Dhel, *D. helophoroides* (Coccinelloidea); Haxy, *H. axyridis* (Coccinelloidea); Nves, *Nicrophorus vespilloides* (Staphylinoidea); Hobl, *Holotrichia oblita* (Scarabaeoidea); Rdom, *Rhyzopertha dominica* (Bostrichoidea); Cbow, *Colaphellus bowringi* (Chrysomeloidea); Cfor, *Cylas formicarius* (Curculionoidea); Atum, *Aethina tumida* (Cucujoidea); Tcas, *Tribolium castaneum* (Tenebrionoidea). Each species is marked with one color in the outer circle. Red and blue leaves are used to mark the OBPs of *M. alternatus* and *D. helophoroides*, respectively. Red branches and light orange leaf background represent the four clusters with high bootstrap support (≥70) containing orthologous OBPs from *M. alternatus* and *D. helophoroides* (MaltOBP24&DhelOBP16, MaltOBP19&DhelOBP22, MaltOBP16&DhelOBP16, MaltOBP10&DhelOBP13), which are marked with A–D.

classified into three types: Classic OBPs, which contain six conserved cysteines; Minus-C OBPs, which have four or five conserved cysteines; and Plus-C OBPs, which exhibit at least two additional cysteines and a conserved proline (Hekmat-Scafe et al., 2002; Xu et al., 2003; Zhou et al., 2004). Alignment of amino acid sequences with AgamOBP48 (a typical Plus-C OBP) from *Anopheles gambiae* showed MaltOBP24, DhelOBP10 and other Coleoptera OBPs from the same clade had eight conserved Cys residues and one conserved Pro residue, belonging to the Plus-C OBP subfamily (Figure S1B). Sequence motifs are one of the basic functional units of molecular evolution, and the high similarity in motif structures among these homologous OBPs implies their potential to bind with similar ligands (Figure S2) (Bailey et al., 2015).

The high-level expression of MaltOBP24 and DhelOBP10 in adult antennae indicated that they are involved in olfactory recognition (Figure 3). Moreover, highly expressed MaltOBP24 in *M. alternatus* 8 days adults

Table 1. Analyses of clade selection pressure and comparison of models of codon evolution by likelihood ratio test (LRT)

Clade ID	Model	NSsites	Parameters	ln L^a	2Δln L^b	p value
A	M0	0	$\omega = 0.038$			
	M1a	1	$p_0 = 0.867$; $\omega_0 = 0.024$	−4,770.461	0	1
	M2a	2	$p_0 = 0.867$; $p_2 = 0$; $\omega_0 = 0.024$; $\omega_2 = 175.282$	−4,770.461		
	M7	7	$p = 0.933$; $q = 18.569$	−4,713.350	0.092	0.955
	M8	8	$p_0 = 0.994$; $p = 0.950$; $q = 19.307$; $\omega = 1.855$	−4,713.304		
B	M0	0	$\omega = 0.005$			
	M1a	1	$p_0 = 0.795$; $\omega_0 = 0.007$	−2,787.063	0	1
	M2a	2	$p_0 = 0.795$; $p_2 = 0.205$; $\omega_0 = 0.007$; $\omega_2 = 1.000$	−2,787.063		
	M7	7	$p = 1.139$; $q = 99.000$	−2,783.648	2.342	0.310
	M8	8	$p_0 = 0.887$; $p = 1.622$; $q = 99.000$; $\omega = 2.774$	−2,782.477		
C	M0	0	$\omega = 0.032$			
	M1a	1	$p_0 = 0.947$; $\omega_0 = 0.026$	−2,108.596	0	1
	M2a	2	$p_0 = 0.947$; $p_2 = 0$; $\omega_0 = 0.026$; $\omega_2 = 1.000$	−2,108.596		
	M7	7	$p = 0.966$; $q = 21.633$	−2,083.457	0	1
	M8	8	$p_0 = 0.999$; $p = 0.966$; $q = 21.635$; $\omega = 3.387$	−2,083.457		
D	M0	0	$\omega = 0.023$			
	M1a	1	$p_0 = 0.912$; $\omega_0 = 0.022$	−2,904.916	0	1
	M2a	2	$p_0 = 0.912$; $p_2 = 0$; $\omega_0 = 0.022$; $\omega_2 = 435.533$	−2,904.916		
	M7	7	$p = 1.356$; $q = 40.260$	−2,887.116	6.916	0.031
	M8	8	$p_0 = 0.954$; $p = 1.733$; $q = 57.043$; $\omega = 1.000$	−2,883.658		

The models and parameters follow the same naming as in the PAML manual, version 4.9j (2020).

^{a}ln(likelihood) value.
^{b}Twice the difference of ln(likelihood) value between the two models compared.

revealed that it might play a role in the process of host conversion from fresh pine trees to stressed pine trees. The highly expressed DhelOBP10 in *D. helophoroides* unmated adults implied its potential function of host location in wide range.

Binding properties of MaltOBP24 and DhelOBP10 with host plant volatiles *in vitro*

Competitive fluorescence-binding assays and fluorescence-quenching assays are combinedly utilized to detect ligand-binding affinities using purified proteins (Figure S3). In the present study, we consider the ligand-binding affinity with OBPs as high if the Ki values <20 μM and weak if Ki > 20 μM (Figure S4). Although several ligands show high binding abilities with OBPs in competitive fluorescence-binding assays (Table 3), fluorescence-quenching assays show that the interaction between most of ligands and OBPs are molecular collisions instead of effective binding (Table S2). For example, high binding affinities are shown between (+)-α-pinene and MaltOBP24 (Ki = 12.83 μM) or (+)-α-longipinene and DhelOBP10 (Ki = 11.47 μM) in fluorescence-binding assays, whereas in the fluorescence-quenching assays, the increasing value of K_{sv} with increasing temperature indicates that their interactions are dynamic quenching—molecular collisions are promoted by higher temperature. By combining the results of these two experiments, it was found that (+)-fenchone, α-terpinolene, 3-carene show high binding affinities with MaltOBP24 and DhelOBP10 in fluorescence-binding assays according to the relatively low dissociation constant (Ki < 20 μM) (Table 3, Figure 4A). In addition, the fluorescence-quenching spectra assays show that their interactions are static quenching according to the decreasing value of K_{sv} with increasing temperature, resulting from the high-temperature damage to the ligand–protein interaction (Table 4, Figure 4B).

Furtherly, based on the double logarithm equation, both n (the number of binding sites per protein) and K_a (apparent association constant) at different temperatures were obtained (Table 4). The values of n are close to 1, which illustrates that the stoichiometry of the binding of (+)-fenchone, α-terpinolene, or 3-carene with MaltOBP24 or DhelOBP10 was 1:1. Then, the thermodynamic equation was used to assess the binding force between these ligands and OBPs. The main acting forces between them are the same: between (+)-fenchone and MaltOBP24 or DhelOBP10 is hydrophobic, as ΔH is > 0 and ΔS is > 0; between

Table 2. Analyses of pairwise protein sequences and evolutionary rate of OBPs from *M. alternatus* and *D. helophoroides*

Pairwise protein sequences	Identity	Similarity	n_{aa}	d_{aa}	p_{aa}	K_{aa}
MaltOBP24&DhelOBP10	50.0%	68.1%	217	101	0.465	0.625
MaltOBP19&DhelOBP22	36.5%	60.0%	186	113	0.608	0.936
MaltOBP16&DhelOBP16	51.6%	73.8%	121	58	0.479	0.652
MaltOBP10&DhelOBP13	44.2%	67.5%	117	64	0.547	0.792

n_{aa} is the total number of amino acid sites in two polypeptide chains compared with each other (excluding deletions and insertions); d_{aa} is the number of sites where they are different; K_{aa} means the number of substitutions per amino acid site over the whole evolutionary period that separated these two polypeptides, $K_{aa} = -\ln(1-p_d)$, where $p_d = d_{aa}/n_{aa}$ is the fraction of different sites.

α-terpinolene or 3-carene and MaltOBP24 or DhelOBP10 is electrostatic force, as ΔH is < 0 and ΔS is > 0 (Table 4). Besides the above three volatiles, DhelOBP10 shows effective binding and high affinity with R-(+)-limonene, whereas MaltOBP24 did not (Table 3, Figures 4A and 4B). These results imply that MaltOBP24 and DhelOBP10 may function in recognition of (+)-fenchone, α-terpinolene, and 3-carene for *M. alternatus* and *D. helophoroides* adults, respectively. DhelOBP10 also functions in the recognition of R-(+)-limonene for *D. helophoroides*.

Detection of behaviorally active compounds

Based on the binding properties, (+)-fenchone, α-terpinolene, 3-carene, and R-(+)-limonene were selected for the behavioral test by Y-tube olfactometer bioassays and RNAi experiment. As for *M. alternatus* adults, only (+)-fenchone could attract adults and 3-carene, α-terpinolene, or R-(+)-limonene did not affect their behavior (Figures 5A, 5B, 5C and 5D), which is consistent with the result of previous studies (Fan et al., 2007b). As for *D. helophoroides* adults, they did not show preference for α-terpinolene (Figure 5C), but showed a significant preference for (+)-fenchone, 3-carene, and R-(+)-limonene (Figures 5A, 5B, and 5D). Further RNAi experiments show that when MaltOBP24 and DhelOBP10 are silenced, attraction indexes of (+)-fenchone to *M. alternatus* and *D. helophoroides* were significantly decreased compared with the non-injected and dsGFP controls (Figures S5 and 5A). Therefore, we suggest that MaltOBP24 and DhelOBP10 play an essential role in the olfactory recognition of (+)-fenchone for *M. alternatus* and *D. helophoroides,* respectively.

Previous studies have reported that 3-carene was the main component of herbivore-induced plant volatiles and had the highest relative amount in the extract of pine wood with longicorn larval tunnels (Pan et al., 2020; Wei et al., 2008). Our results showed that RNAi of DhelOBP10 led to a significantly lower attraction index of 3-carene for *D. helophoroides* (Figure 5B), which indicates that DhelOBP10 works in recognizing 3-carene and locating the habitat of host cerambycid beetles. The attractive trend for R-(+)-limonene was not altered by silencing DhelOBP10 (Figure 5D), which implies that the recognition of R-(+)-limonene may be a result of the combinatorial action of multiple OBPs in *D. helophoroides* (Swarup et al., 2011).

Identifying evolutionarily conserved OBPs by phylogenetic analysis upon common herbivorous insects and enemies

OBPs from six pairs of common herbivorous insects and enemies were selected to perform phylogenetic analysis: in the forest ecosystem, *M. alternatus* (Coleoptera)–*D. helophoroides* (Coleoptera, parasitical enemy), *Dendrolimus punctatus* (Lepidoptera)–*Trichogramma dendrolimi* (Hymenoptera, parasitical enemy); in the filed ecosystem, *N. lugens* (Hemiptera) –*Cyrtorhinus lividipennis* (Hemiptera, predacity enemy), *S. avenae* (Hemiptera)–*E. balteatus* (Diptera, predacity enemy), *Plutella xylostella* (Lepidoptera)–*Cotesia vestalis* (Hymenoptera, parasitical enemy), *Euschistus heros* (Hemiptera)–*Telenomus podisi* (Hymenoptera, parasitical enemy). Moreover, two euryphagic predators, *H. axyridis* (Coleoptera) and *C. pallens* (Neuroptera), are the natural enemies of *S. avenae* and *P. xylostella*. There were 13 pairs of OBPs belonging to herbivores and their natural enemies in the same clusters with high bootstrap support (≥70). In general, these OBPs exist no matter in forest ecosystem or field ecosystem, in predation or parasitic relations. And the herbivores and enemies from the same order are more likely to share more, for instance, *M. alternatus* and *D. helophoroides*, *N. lugens* and *C. lividipennis* with four and two pairs, respectively. Same-cluster OBPs are also existing in the herbivores and their enemies from different orders,
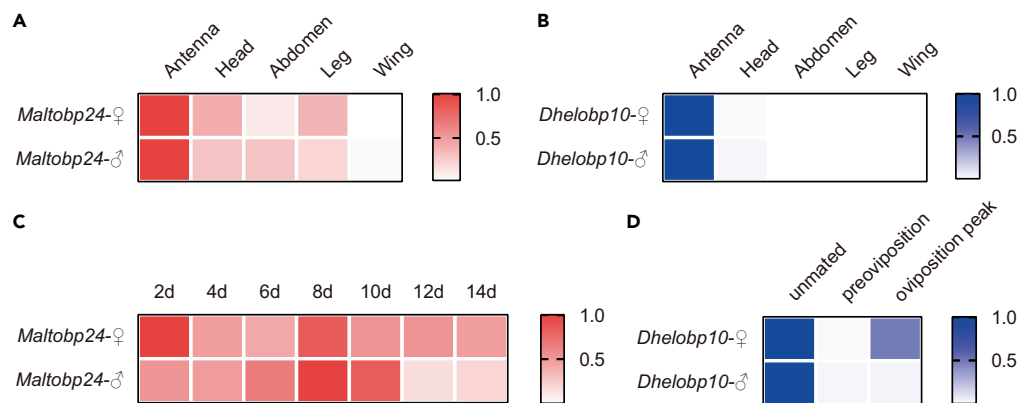
Figure 3. Expression profiles of MaltOBP24 and DhelOBP10

(A and B) Relative mRNA expression level of MaltOBP24 in different tissues of 8-day *M. alternatus* adults (A) and DhelOBP10 in different tissues of unmated *D. helophoroides* adults (B).

(C and D) Relative mRNA expression level of MaltOBP24 at different developmental stages in the antennae of *M. alternatus* adults (C) and DhelOBP10 at different developmental stages in the antennae of *D. helophoroides* adults (D).

including SaveOBP3/EbalOBP3 in *S. avenae* and *E. balteatus*; SaveOBP3/HaxyOBP3 in *S. avenae* and *H. axyridis*; SaveOBP4/HaxyOBP6 in *S. avenae* and *H. axyridis*; SaveOBP4/CpalOBP11 in *S. avenae* and *C. pallens*; EherOBP1/TpodOBP2 in *E. heros* and *T. podisi*; PxylOBP3/HaxyOBP6 in *P. xylostella* and *H. axyridis*; PxylOBP3/CpalOBP11 in *P. xylostella* and *C. pallens* (Figure 6). Each pair of OBPs (excluding OBPs from *M. alternatus* and *D. helophoroides*) shared high identity (41.7–97.5%) and similarity (51.9–98.3%) based on amino acid sequences without signal peptide and $\omega < 1$ indicated they have evolved under purifying selection (Table S3).

DISCUSSION

In-depth function research on the evolutionarily conserved OBPs from herbivores and enemies will help us to better understand the olfactory molecular mechanism of the co-evolution relationship existing in tritrophic interactions. Our study affirms that evolutionarily conserved MaltOBP24 from *Monochamus alternates* and DhelOBP10 from *D. helophoroides* can participate in establishing tritrophic interactions through recognizing (+)-fenchone from stressed pines, which works in guiding the herbivore and enemy to locate the same spawning place. Many pieces of research showed that plant volatiles can be used not only by herbivorous insects to find their host plants, but also by the natural enemies of the herbivores to find their prey, especially when serving as attractants over a larger spatial range (Dethier, 1982; Halitschke et al., 2008; Ode, 2006; Visser, 1988; Xu and Turlings, 2018). *M. alternates* adult activity patterns can be characterized by alternate dispersal between the healthy food plants and the stressed host plants where they mate and oviposit. Newly emerging *M. alternates* adults from dead host pine trees disperse to fresh twigs for maturation feeding. When reaching sexual maturity, they need to aggregate on dying pine trees for copulation and oviposition because their larvae can only survive in suppressed pines with weak resistance (Akbulut and Stamps, 2012; Fan et al., 2007a; Fauziah et al., 1987; Hanks, 1999; Maehara et al., 2015). *D. helophoroides* is an ectoparasitoid beetle whose larvae parasitize late-instar larvae, pupae, and pharate adults of *M. alternates*. To localize *M. alternates* in natural habitats in time, *D. helophoroides* adults must make full use of the numerous chemical cues of the multitrophic environment. For their long-distance disperse, volatiles from stressed pines infested by *M. alternates* play an essential role (Haverkamp et al., 2018; Urano, 2003; Wei et al., 2009). It has been estimated that *M. alternatus*, *D. helophoroides*, and *Pinus massoniana* (a typical host pine) had already existed in the Paleogene Period, which implies that their interactions may last for a long time (Ashman et al., 2021; Eckert and Hall, 2006; McKenna et al., 2019; Saladin et al., 2017).

Previous studies have shown that (+)-α-pinene, the amount of which greatly increased when the pines were stressed, may be an important element for both *M. alternatus* and *D. helophoroides* in host location via olfaction (Fan et al., 2007a, 2007b; Ren et al., 2017). However, the molecular mechanism for the recognition of the same volatile by *M. alternatus* and *D. helophoroides* has not been reported. In this study, we proved that (+)-fenchone emitted by stressed pine trees can take part in establishing tritrophic interactions through attracting both mature adults of *M. alternatus* and *D. helophoroides*. Fenchone has been reported

Table 3. Dissociation constants (Ki) of 14 ligands and MaltOBP24/DhelOBP10 in neutral pH and acid pH environment (unit: μM)

Ligands	MaltOBP24 Ki (μmol/L)		DhelOBP10 Ki (μmol/L)	
	pH7.4	pH5.0	pH7.4	pH5.0
(+)-fenchone	13.69 ± 0.72	32.01 ± 3.30	16.93 ± 1.83	13.87 ± 0.29
α-terpinolene	13.65 ± 1.08	>50	19.19 ± 0.48	12.79 ± 3.17
3-carene	3.31 ± 0.68	23.47 ± 2.33	14.55 ± 2.61	13.86 ± 2.91
R-(+)-limonene	>50	>50	12.68 ± 1.82	3.87 ± 0.08
S-(−)-limonene	>50	>50	17.27 ± 1.53	10.07 ± 1.93
(+)-limonene oxide	37.67 ± 5.37	>50	27.71 ± 4.92	6.00 ± 2.63
camphene	22.05 ± 3.21	>50	24.46 ± 2.44	8.29 ± 1.99
camphor	>50	>50	33.75 ± 1.04	9.09 ± 1.70
β-caryophyllene	–	–	–	–
(−)-caryophyllene oxide	24.23 ± 1.94	38.51 ± 3.44	15.66 ± 1.26	3.65 ± 0.34
(+)-α-longipinene	44.84 ± 7.23	–	11.47 ± 1.21	9.86 ± 0.45
myrcene	24.318 ± 3.95	22.37 ± 2.29	28.70 ± 1.12	3.93 ± 0.71
(+)-α-pinene	12.83 ± 1.09	33.96 ± 7.02	22.04 ± 1.37	4.45 ± 2.55
(+)-β-pinene	>50	>50	22.42 ± 2.43	8.76 ± 0.33

The dissociation constants (Ki) of 14 common volatiles from forest to MaltOBP24 and DhelOBP10 were calculated. If Ki < 20 μM, it was considered the ligand-binding affinity was high, and low if Ki > 20 μM. Data values represent the mean ± SEM.

to be preserved in late Oligocene resin, suggesting its potential to mediate this tritrophic interaction over a long time span (Paul et al., 2020). Interestingly, at the molecular level, we find that (+)-fenchone cannot be detected successfully for both *M. alternatus* and *D. helophoroides* without a pair of evolutionarily conserved OBPs – MaltOBP24 and DhelOBP10. This finding introduces a new concept to understand the form of tritrophic interactions: the evolutionarily conserved OBPs from herbivores and their enemies could take part in the critical stage of building tritrophic interactions by specifically binding with the same volatiles from plant hosts.

Phylogenetic trees reveal that most OBPs of *M. alternatus*, *D. helophoroides* and other insects are arranged in different clusters, which implies their functional diversity in various physiological processes. The current size of OBPs might result from adaptive changes fostered by ecological shifts. Most OBPs are arranged in multiple small clusters with species-specific radiations, which is often strongly related with adaption to ecological niches and speciation (Vieira and Rozas, 2011; Wang et al., 2019). Belonging to the same order – Coleoptera, *M. alternatus*, and *D. helophoroides* share more pairs of evolutionarily conserved OBPs than those from distinct orders, which is in accordance with the law of evolution (Hansson and Stensmyr, 2011; Xu et al., 2009). Under constant selective pressure and a complex environment, such high conservation of OBPs may suggest their essential role in herbivore-enemy coexistence relationships over long timescales via olfaction (Farias et al., 2015; Vandermoten et al., 2011). Future studies on the other three pairs of evolutionarily conserved OBPs from *M. alternatus* and *D. helophoroides* will provide us more information. The clusters with conserved MaltOBPs and DhelOBPs also contain OBPs from other families in Coleoptera, especially the conserved lineage with MaltOBP24 and DhelOBP10, which is the only cluster containing OBPs from all tested superfamilies. Such high conservation over millions of years may suggest a key conserved function among Coleoptera (Zhang et al., 2018).

Functional differentiation of evolutionarily conserved OBP genes is another important aspect for ecological adaptation. The research on paralogs of the *Drosophila melanogaster* Obp50a–d gene cluster revealed functional diversification within the Obp50 cluster with Obp50a contributing to development and Obp50-days to stress resistance (Johnstun et al., 2021). Many studies have shown that single or several amino acid substitutions can alter the function of one OBP. The site-specific changes in the plus-C OBP50a would likely promote structural and functional changes in *Anastrepha fraterculus* and *Anastrepha obliqua* (Campanini
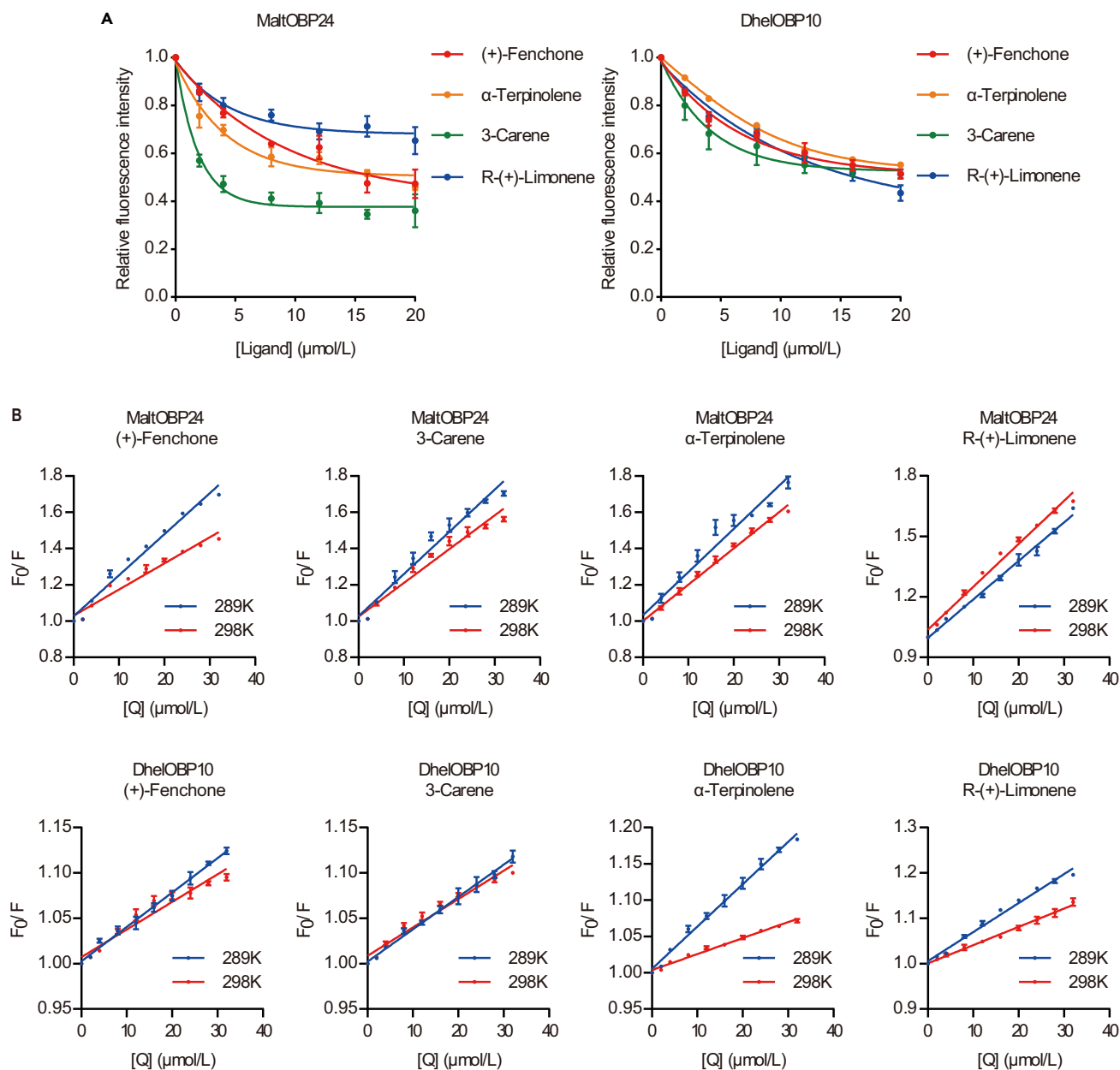
Figure 4. Binding properties of MaltOBP24 and DhelOBP10 with host plant volatiles in vitro

(A) Competitive binding curves of MaltOBP24-1-NPN complex and DhelOBP10-1-NPN complex to (+)-fenchone, 3-carene, α-terpinolene, R-(+)-limonene in neutral pH environment. The affinity of binding of MaltOBP24 and DhelOBP10 were measured using the 1-NPN fluorescence probe. The fluorescent signal is reported as a function of the ligand concentration. A decrease in fluorescence intensity of 1-NPN with increasing concentrations of binding ligands is seen. There is a clear difference in affinities between R-(+)-limonene and the other three ligands as for MaltOBP24.

(B) Fluorescence quenching analyses of MaltOBP24 and DhelOBP10 with (+)-fenchone, 3-carene, α-terpinolene, R-(+)-limonene in a neutral pH environment. The linear Stern-Volmer plots at high (298 K) and low temperatures (289 K) are shown in blue and red, respectively. The slope of them (K_{sv}) decreased when temperature increased (289–298 K), indicating that static quenching occurred when MaltOBP24 interacted with (+)-fenchone, 3-carene, and α-terpinolene, and when DhelOBP10 interacted with (+)-fenchone, 3-carene, α-terpinolene, R-(+)-limonene. The slope increased with an increase in the temperature, indicating that dynamic quenching occurred when MaltOBP24 interacted with R-(+)-limonene. K_{sv}, quenching constant; T, temperature; F_0 and F are the fluorescence intensity in the absence or presence of a quencher at concentration [Q]. The error bars represent ± SEM.

Table 4. Calculations of the static quenching analyses of MaltOBP24 and DhelOBP10

Ligands	T (K)	K_{sv} (L·mol⁻¹)	K_q (L·mol⁻¹·s⁻¹)	R^2	n	K_a (L·mol⁻¹)	R^2	ΔG (J·mol⁻¹)	ΔH (J·mol⁻¹)	ΔS (J·mol⁻¹)
MaltOBP24-pH 7.4										
(+)-fenchone	289	24,531 ± 303.9	2.4531×10^{12}	0.9846	0.9696 ± 0.0159	3,312,799.36	0.9526	−36,073.16	126.84	125.26
	298	14,813 ± 141.8	1.4813×10^{12}	0.9666	0.9369 ± 0.0424	2,154,595.09	0.9241	−36,130.71		
α-terpinolene	289	25,179 ± 659.6	2.5179×10^{12}	0.9751	1.0017 ± 0.0270	5,449,703.40	0.9344	−37,269.17	−1,607.15	123.40
	298	20,347 ± 501.6	2.0347×10^{12}	0.9868	0.9459 ± 0.0139	2,525,092.74	0.9311	−36,523.84		
3-carene	289	24,156 ± 442.5	2.4156×10^{12}	0.9510	1.0464 ± 0.0461	9,394,307.39	0.9099	−38,577.56	−2,845.48	123.64
	298	18,949 ± 876.5	1.8949×10^{12}	0.9606	0.9645 ± 0.090	3,347,243.70	0.9147	−37,222.17		
DhelOBP10-pH 7.4										
(+)-fenchone	289	3,742 ± 92.59	3.742×10^{11}	0.9726	0.9404 ± 0.0271	2,071.51	0.9544	−18,347.45	2,134.30	70.87
	298	2,913 ± 190.8	2.913×10^{11}	0.9334	0.9471 ± 0.0676	2,011.77	0.9729	−18,846.32		
α-terpinolene	289	5,736 ± 153.1	5.736×10^{11}	0.9852	1.0321 ± 0.0670	8,904.93	0.9650	−21,851.44	−11,356.86	36.31
	298	2,139 ± 58.09	2.139×10^{11}	0.9826	0.9823 ± 0.1034	2,093.14	0.9485	−18,944.55		
3-carene	289	3,524 ± 122.4	3.524×10^{11}	0.9649	0.9999 ± 0.0605	3,729.25	0.9746	−19,760.09	−7,595.91	42.09
	298	2,970 ± 15.32	2.970×10^{11}	0.9578	0.9088 ± 0.0218	1,407.15	0.9504	−17,960.72		
R-(+)-limonene	289	6,287 ± 91.45	6.287×10^{11}	0.9815	0.9715 ± 0.0292	4,986.95	0.9803	−20,458.37	−6,986.94	46.61
	298	4,016 ± 108.1	4.016×10^{11}	0.9621	0.9324 ± 0.0422	1,925.95	0.9713	−18,738.30		

Static quenching analyses of MaltOBP24 with (+)-fenchone, α-terpinolene, 3-carene and DhelOBP10 with (+)-fenchone, α-terpinolene, 3-carene, R-(+)-limonene, including the quenching constant (K_{sv}), the bimolecular quenching constant (K_q), the apparent association constant (K_a), the number of binding sites (n), and the free energy change (ΔG), enthalpy change (ΔH), and entropy change (ΔS) at different temperatures in neutral pH. Data values represent the mean ± SEM.
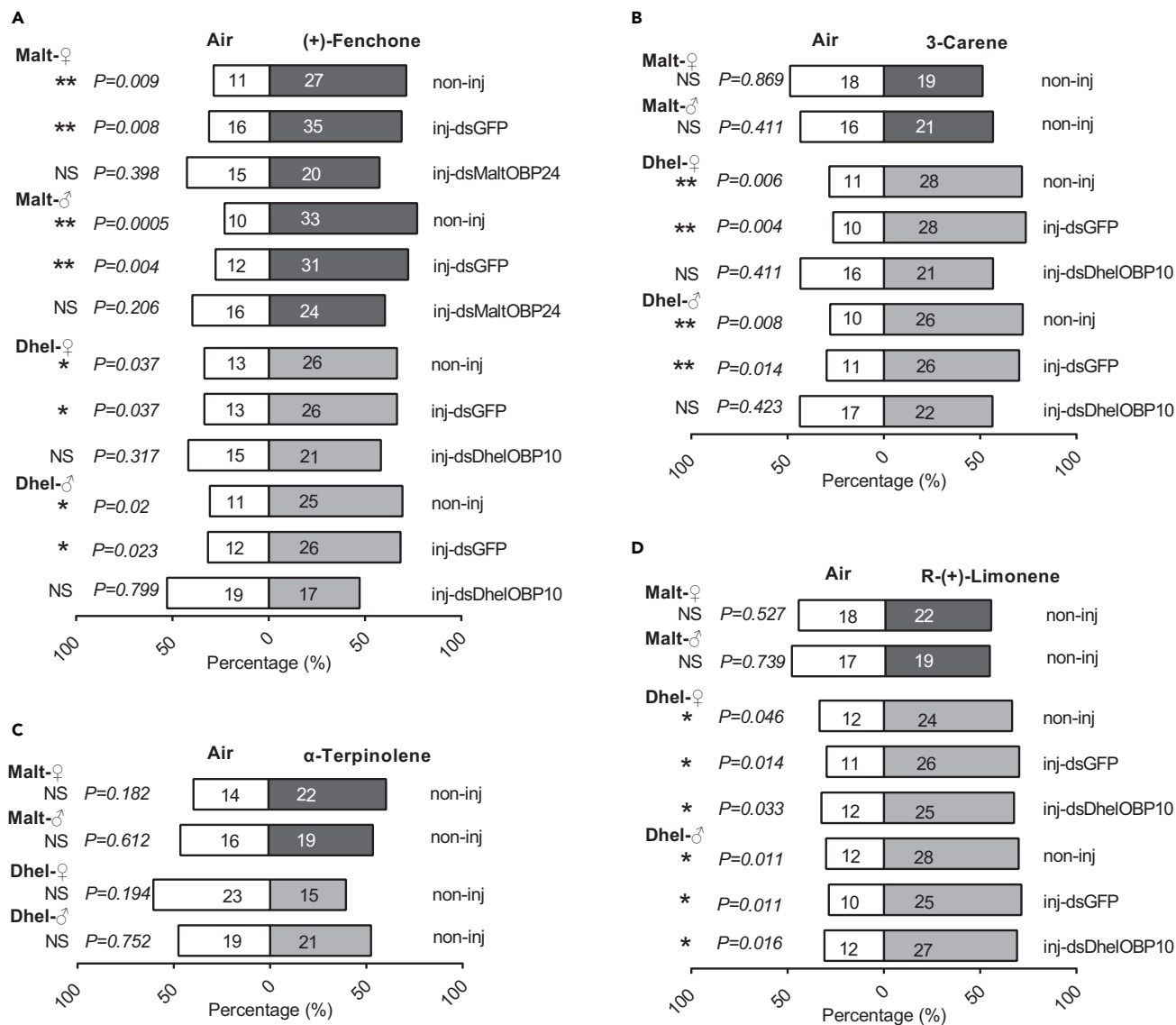
Figure 5. Y-tube olfactometer bioassays

(A–D) Behavioral responses of 8-day *M. alternatus* adults and unmated *D. helophoroides* adults with different treaments to (+)-Fenchone (A), α-Terpinolene (B), 3-Carene (C), R-(+)-Limonene (D).

Selectivity represented the percentage of beetles with credible behavior choices. The number in the column indicated the total number of beetles choosing the arm. "*" indicated $p < 0.05$; "**" indicated $p < 0.01$; "NS" indicated there was no significant differences. p-values were determined by the Chi-square test.

and de Brito, 2016). Despite their relatively high sequence identity, different functional properties between MaltOBP24 and DhelOBP10 have also been found in our study. Notably, the results of fluorescence assays reveal that DhelOBP10 can bind with R-(+)-limonene effectively, whereas MaltOBP24 can not. These differences may contribute to their respective ecological adaptions.

Overall, the connections between the divergence and conservation in the evolution of OBPs and environmental adaptions are complex and varied. Our research provides a worthy perspective on understanding the olfactory genetic basis of tritrophic co-evolution.

Limitations of the study

Whereas the functional tests of the two orthologous OBPs (MaltOBP24 and DhelOBP10) were performed rigorously, it is not certain that the function of (+)-fenchone binding is conserved or evolves independently,
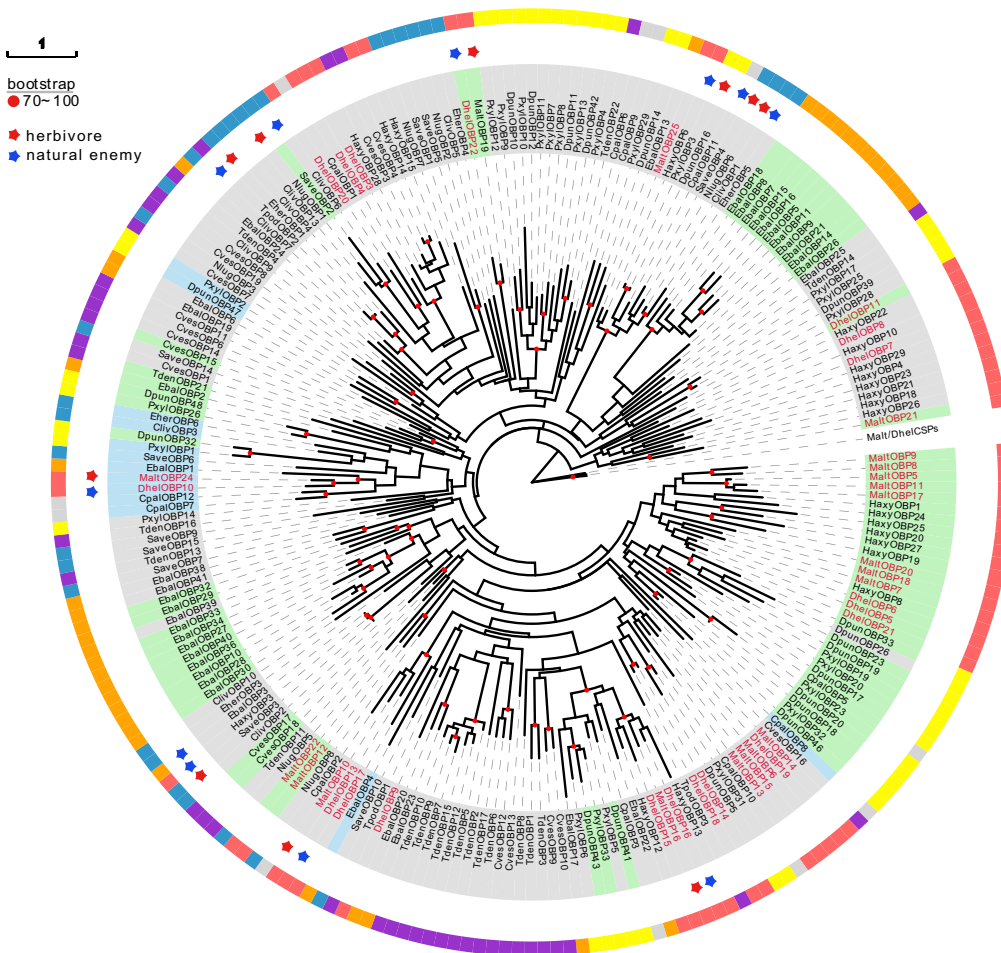
Figure 6. Phylogenetic analysis of OBPs from common herbivorous insects and enemies

The phylogenetic tree is built using the amino acid sequences without signal peptides of 234 OBPs from fourteen species belonging to six orders and 13 CSPs from *M. alternatus* and *D. helophoroides* based on the maximum likelihood algorithm. Bootstrap values larger than 70 are labeled with red dots on the nodes. The protein names and sequences used in this analysis are listed in a supplemental information. Malt, *M. alternatus*; Dhel, *D. helophoroides*; Haxy, *H. axyridis*; Save, *S. avenae*; Nlug, *N. lugens*; Cliv, *C. lividipennis*; Eher, *E. heros*; Pxyl, *P. xylostella*; Dpun, *D. punctatus*; Cves, *C. vestalis*; Tden, *T. dendrolimi*; Tpod, *T. podisi*; Ebal, *E. balteatus*; Cpal, *C. pallens*. The outer circle indicates the different orders (Coleoptera-red, Hemiptera-blue, Lepidoptera-yellow, Hymenoptera-purple, Diptera-orange, Neuroptera-grey). The leaf background is color coded for each subfamily (Classic OBPs-grey, Plus-C OBPs-blue, Minus-C OBPs-green). Stars are used to mark 13 pairs of OBPs belonging, respectively, to herbivores (labeled with red star) and their natural enemies (labeled with blue star) existing in the same clusters with high bootstrap support (≥70): MaltOBP24/DhelOBP10, MaltOBP16/DhelOBP16, MaltOBP10/DhelOBP13, MaltOBP19/DhelOBP22 in *M. alternatus* and *D. helophoroides*; NlugOBP1/ClivOBP6, NlugOBP6/ClivOBP1, in *N. lugens* and *C. lividipennis*; SaveOBP3/EbalOBP3 in *S. avenae* and *E. balteatus*; SaveOBP3/HaxyOBP3 in *E. balteatus* and *H. axyridis*; EherOBP1/TpodOBP2 in *E. heros* and *T. podisi*; PxylOBP3/CpalOBP11 in *P. xylostella* and *C. pallens. M. alternatus* and *D. helophoroides, N. lugens* and *C. lividipennis* are from the same order, and other herbivores and their natural enemies are from different orders.

only depending on the findings of this study. In addition, high conservation in the lineage of MaltOBP24, DhelOBP10, and OBPs from other families among Coleoptera implies some key conserved functions associated with the evolution of Coleoptera, but there is no further exploration in this study.

STAR★METHODS

Detailed methods are provided in the online version of this paper and include the following:

- KEY RESOURCES TABLE
- RESOURCE AVAILABILITY

SUPPLEMENTAL INFORMATION

Supplemental information can be found online at https://doi.org/10.1016/j.isci.2022.104664.

AUTHOR CONTRIBUTIONS

M.Q.W. designed and supervised the project. R.N.Y., D.Z.L., and S.C.Y. performed the experiments. R.N.Y. interpreted the results and analyzed the data. M.Q.W., R.N.Y., and D.Z.L. co-wrote the manuscript.

DECLARATION OF INTERESTS

The authors declare no competing interests.

REFERENCES

Aartsma, Y., Bianchi, F.J.J.A., van der Werf, W., Poelman, E.H., and Dicke, M. (2017). Herbivore-induced plant volatiles and tritrophic interactions across spatial scales. New Phytol. *216*, 1054–1063. https://doi.org/10.1111/nph.14475.

Ache, B.W., and Young, J.M. (2005). Olfaction: diverse species, conserved principles. Neuron *48*, 417–430. https://doi.org/10.1016/j.neuron.2005.10.022.

Akbulut, S., and Stamps, W.T. (2012). Insect vectors of the pinewood nematode: a review of the biology and ecology of Monochamus species. Forest Pathol. *42*, 89–99. https://doi.org/10.1111/j.1439-0329.2011.00733.x.

Ashman, L.G., Shin, S., Zwick, A., Slipinski, A., and McKenna, D.D. (2021). The first phylogeny of Australasian Lamiinae longhorn beetles (Coleoptera: Cerambycidae) reveals poor tribal classification and a complex biogeographic history. Syst. Entomol. *47*, 213–230.

Bailey, T.L., Johnson, J., Grant, C.E., and Noble, W.S. (2015). The MEME suite. Nucleic Acids Res. *43*, W39–W49. https://doi.org/10.1093/nar/gkv416.

Beale, M.H., Birkett, M.A., Bruce, T.J.A., Chamberlain, K., Field, L.M., Huttly, A.K., Martin, J.L., Parker, R., Phillips, A.L., Pickett, J.A., et al.

(2006). Aphid alarm pheromone produced by transgenic plants affects aphid and parasitoid behavior. Proc. Natl. Acad. Sci. USA *103*, 10509–10513. https://doi.org/10.1073/pnas.0603998103.

Brito, N.F., Moreira, M.F., and Melo, A.C. (2016). A look inside odorant-binding proteins in insect chemoreception. J. Insect Physiol. *95*, 51–65. https://doi.org/10.1016/j.jinsphys.2016.09.008.

Bruce, T.J., Wadhams, L.J., and Woodcock, C.M. (2005). Insect host location: a volatile situation. Trends Plant Sci. *10*, 269–274. https://doi.org/10.1016/j.tplants.2005.04.003.

Campanacci, V., Krieger, J., Bette, S., Sturgis, J.N., Lartigue, A., Cambillau, C., Breer, H., and Tegoni, M. (2001). Revisiting the specificity of Mamestra brassicae and Antheraea polyphemus pheromone-binding proteins with a fluorescence binding assay. J. Biol. Chem. *276*, 20078–20084. https://doi.org/10.1074/jbc.m100073200.

Campanini, E.B., and de Brito, R.A. (2016). Molecular evolution of Odorant-binding proteins gene family in two closely related Anastrepha fruit flies. BMC Evol. Biol. *16*, 198. https://doi.org/10.1186/s12862-016-0775-0.

Carey, A.F., Wang, G.R., Su, C.Y., Zwiebel, L.J., and Carlson, J.R. (2010). Odorant reception in the malaria mosquito Anopheles gambiae. Nature *464*, 66–71. https://doi.org/10.1038/nature08834.

Dani, F.R., Iovinella, I., Felicioli, A., Niccolini, A., Calvello, M.A., Carucci, M.G., Qiao, H.L., Pieraccini, G., Turillazzi, S., Moneti, G., and Pelosi, P. (2010). Mapping the expression of soluble olfactory proteins in the honeybee. J. Proteome Res. *9*, 1822–1833. https://doi.org/10.1021/pr900969k.

de Fouchier, A., Walker, W.B., Montagné, N., Steiner, C., Binyameen, M., Schlyter, F., Chertemps, T., Maria, A., François, M.C., Monsempes, C., et al. (2017). Functional evolution of Lepidoptera olfactory receptors revealed by deorphanization of a moth repertoire. Nat. Commun. *8*, 15709. https://doi.org/10.1038/ncomms15709.

Dethier, V.G. (1982). Mechanism of host-plant recognition. Entomol. Exp. Appl. *31*, 49–56. https://doi.org/10.1111/j.1570-7458.1982.tb03118.x.

Du, Y.J., Poppy, G.M., Powell, W., Pickett, J.A., Wadhams, L.J., and Woodcock, C.M. (1998). Identification of semiochemicals released during aphid feeding that attract parasitoid Aphidius ervi. J. Chem. Ecol. *24*, 1355–1368. https://doi.org/10.1023/a:1021278816970.

Eckert, A.J., and Hall, B.D. (2006). Phylogeny, historical biogeography, and patterns of diversification for Pinus (Pinaceae): phylogenetic tests of fossil-based hypotheses. Mol. Phylogenet. Evol. *40*, 166–182. https://doi.org/10.1016/j.ympev.2006.03.009.

Fan, J.T., Kang, L., and Sun, J.H. (2007a). Role of host volatiles in mate location by the Japanese pine sawyer, Monochamus alternatus Hope (Coleoptera : Cerambycidae). Environ. Entomol. *36*, 58–63. https://doi.org/10.1093/ee/36.1.58.

Fan, J.T., Sun, J.H., and Shi, J. (2007b). Attraction of the Japanese pine sawyer, Monochamus alternatus, to volatiles from stressed host in China. Ann. For. Sci. *64*, 67–71. https://doi.org/10.1051/forest:2006089.

Farias, L.R., Schimmelpfeng, P.H.C., Togawa, R.C., Costa, M.M.C., Grynberg, P., Martins, N.F., Borges, M., Blassioli-Moraes, M.C., Laumann, R.A., Báo, S.N., and Paula, D.P. (2015). Transcriptome-based identification of highly similar odorant-binding proteins among neotropical stink bugs and their egg parasitoid. PLoS One *10*, e0132286. https://doi.org/10.1371/journal.pone.0132286.

Fauziah, B.A., Hidaka, T., and Tabata, K. (1987). The reproductive behavior of Monochamus alternatus Hope (Coleoptera: Cerambycidae). Appl. Entomol. Zool. *22*, 272–285. https://doi.org/10.1303/aez.22.272.

Goldman, N., and Yang, Z.H. (1994). A codon-based model of nucleotide substitution for protein-coding DNA sequences. Mol. Biol. Evol. *11*, 725–736. https://doi.org/10.1093/oxfordjournals.molbev.a040153.

Gu, S.H., Zhou, J.J., Wang, G.R., Zhang, Y.J., and Guo, Y.Y. (2013). Sex pheromone recognition and immunolocalization of three pheromone binding proteins in the black cutworm moth Agrotis ipsilon. Insect Biochem. Mol. Biol. *43*, 237–251. https://doi.org/10.1016/j.ibmb.2012.12.009.

Halitschke, R., Stenberg, J.A., Kessler, D., Kessler, A., and Baldwin, I.T. (2008). Shared signals–'alarm calls' from plants increase apparency to herbivores and their enemies in nature. Ecol. Lett. *11*, 24–34. https://doi.org/10.1111/j.1461-0248.2007.01123.x.

Hanks, L.M. (1999). Influence of the larval host plant on reproductive strategies of cerambycid beetles. Annu. Rev. Entomol. *44*, 483–505. https://doi.org/10.1146/annurev.ento.44.1.483.

Hansson, B.S. (2002). A bug's smell–research into insect olfaction. Trends Neurosci. *25*, 270–274. https://doi.org/10.1016/s0166-2236(02)02140-9.

Hansson, B.S., and Stensmyr, M.C. (2011). Evolution of insect olfaction. Neuron *72*, 698–711. https://doi.org/10.1016/j.neuron.2011.11.003.

Haverkamp, A., Hansson, B.S., and Knaden, M. (2018). Combinatorial codes and labeled lines: how insects use olfactory cues to find and judge food, mates, and oviposition sites in complex environments. Front. Physiol. *9*, 49. https://doi.org/10.3389/fphys.2018.00049.

He, P., Chen, G.L., Li, S., Wang, J., Ma, Y.F., Pan, Y.F., and He, M. (2019). Evolution and functional analysis of odorant-binding proteins in three rice planthoppers: *Nilaparvata lugens*, *Sogatella furcifera*, and *Laodelphax striatellus*. Pest Manag. Sci. *75*, 1606–1620. https://doi.org/10.1002/ps.5277.

He, Z.L., Zhang, H.K., Gao, S.H., Lercher, M.J., Chen, W.H., and Hu, S.N. (2016). Evolview v2: an online visualization and management tool for customized and annotated phylogenetic trees. Nucleic Acids Res. *44*, W236–W241. https://doi.org/10.1093/nar/gkw370.

Hekmat-Scafe, D.S., Scafe, C.R., McKinney, A.J., and Tanouye, M.A. (2002). Genome-wide analysis of the odorant-binding protein gene family in Drosophila melanogaster. Genome Res. *12*, 1357–1369. https://doi.org/10.1101/gr.239402.

Jing, D.P., Zhang, T.T., Prabu, S., Bai, S.X., He, K.L., and Wang, Z.Y. (2020). Molecular characterization and volatile binding properties of pheromone binding proteins and general odorant binding proteins in Conogethes pinicolalis (Lepidoptera: Crambidae). Int. J. Biol. Macromol. *146*, 263–272. https://doi.org/10.1016/j.ijbiomac.2019.12.248.

Johnstun, J.A., Shankar, V., Mokashi, S.S., Sunkara, L.T., Ihearahu, U.E., Lyman, R.L., Mackay, T.F.C., and Anholt, R.R.H. (2021). Functional diversification, redundancy, and epistasis among paralogs of the Drosophila melanogaster Obp50a-d gene cluster. Mol. Biol. Evol. *38*, 2030–2044. https://doi.org/10.1093/molbev/msab004.

Lakowicz, Joseph, R. (2008). Principles of Fluorescence Spectroscopy, Third Edition (Springers).

Kimura, M. (1969). Rate of molecular evolution considered from standpoint of population genetics. Proc. Natl. Acad. Sci. USA *63*, 1181–1188. https://doi.org/10.1073/pnas.63.4.1181.

Kobayashi, F., Yamane, A., Ikeda, T., and YAmAne, A. (1984). The Japanese pine sawyer beetle as the vector of pine wilt disease. Annu. Rev. Entomol. *29*, 115–135. https://doi.org/10.1146/annurev.en.29.010184.000555.

Kumar, S., Stecher, G., Li, M., Knyaz, C., and Tamura, K. (2018). Mega X: molecular evolutionary genetics analysis across Computing platforms. Mol. Biol. Evol. *35*, 1547–1549. https://doi.org/10.1093/molbev/msy096.

Leal, W.S. (2013). Odorant reception in insects: roles of receptors, binding proteins, and degrading enzymes. Annu. Rev. Entomol. *58*, 373–391. https://doi.org/10.1146/annurev-ento-120811-153635.

Li, L., Liu, Z., and Sun, J. (2015). Olfactory cues in host and host-plant recognition of a polyphagous ectoparasitoid Scleroderma guani. Biocontrol *60*, 307–316. https://doi.org/10.1007/s10526-015-9651-x.

Li, Z.Q., Zhang, S., Cai, X.M., Luo, J.Y., Dong, S.L., Cui, J.J., and Chen, Z.M. (2018). Distinct binding affinities of odorant-binding proteins from the natural predator Chrysoperla sinica suggest different strategies-to-hunt-prey. J. Insect Physiol. *111*, 25–31. https://doi.org/10.1016/j.jinsphys.2018.10.004.

Liu, Y.P., Du, L.X., Zhu, Y., Yang, S.Y., Zhou, Q., Wang, G.R., and Liu, Y. (2020). Identification and sex-biased profiles of candidate olfactory genes in the antennal transcriptome of the parasitoid wasp Cotesia vestalis. Comp. Biochem. Physiol. D-Genomics Proteomics *34*, 100657. https://doi.org/10.1016/j.cbd.2020.100657.

Maehara, N., Aikawa, T., and Kanzaki, N. (2015). Relationship between pine wilt disease development in asymptomatic carrier trees of Bursaphelenchus xylophilus (Nematoda: Apelenchoididae) and their use by Monochamus alternatus (Coleoptera: Cerambycidae). Appl. Entomol. Zool. *50*, 33–39. https://doi.org/10.1007/s13355-014-0299-2.

Maida, R., Ziegelberger, G., and Kaissling, K.E. (2003). Ligand binding to six recombinant pheromone-binding proteins of Antheraea polyphemus and Antheraea pernyi. J. Comp. Physiol. B Biochem. Syst. Environ. Physiol. *173*, 565–573. https://doi.org/10.1007/s00360-003-0366-4.

McKenna, D.D., Shin, S., Ahrens, D., Balke, M., Beza-Beza, C., Clarke, D.J., Donath, A., Escalona, H.E., Friedrich, F., Letsch, H., et al. (2019). The evolution and genomic basis of beetle diversity. Proc. Natl. Acad. Sci. USA *116*, 24729–24737. https://doi.org/10.1073/pnas.1909655116.

Mi, F., and Wang, M. (2020). Identification volatile compounds involved in host location by

Dastarcus helophoroides. Chin. J. Biol. Control 36, 685–689.

Nei, M., and Kumar, S. (2000). Molecular Evolution and Phylogenetics (Oxford University Press).

Ode, P.J. (2006). Plant chemistry and natural enemy fitness: effects on herbivore and natural enemy interactions. Annu. Rev. Entomol. 51, 163–185. https://doi.org/10.1146/annurev.ento.51.110104.151110.

Pan, L.N., Xiang, W.F., Sun, Z.Y., Yang, Y.X., Han, J.Y., Wang, Y.H., Yan, C.C., and Li, M. (2020). CcOBP2 plays a crucial role in 3-carene olfactory response of the parasitoid wasp Chouioia cunea. Insect Biochem. Mol. Biol. 117, 103286. https://doi.org/10.1016/j.ibmb.2019.103286.

Paul, S., Gross, D., Bechtel, A., and Dutta, S. (2020). Preservation of monoterpenoids in Oligocene resin: insights into the evolution of chemical defense mechanism of plants in deep-time. Int. J. Coal Geol. 217, 103326. https://doi.org/10.1016/j.coal.2019.103326.

Price, P.W., Bouton, C.E., Gross, P., McPheron, B.A., Thompson, J.N., and Weis, A.E. (1980). Interactions among three trophic levels: influence of plants on interactions between insect herbivores and natural enemies. Annu. Rev. Ecol. Systemat. 11, 41–65. https://doi.org/10.1146/annurev.es.11.110180.000353.

Ren, L.L., Balakrishnan, K., Luo, Y.Q., and Schütz, S. (2017). EAG response and behavioral orientation of Dastarcus helophoroides (Fairmaire) (Coleoptera: Bothrideridae) to synthetic host-associated volatiles. PLoS One 12, e0190067. https://doi.org/10.1371/journal.pone.0190067.

Robertson, H.M., Robertson, E.C.N., Walden, K.K.O., Enders, L.S., and Miller, N.J. (2019). The chemoreceptors and odorant binding proteins of the soybean and pea aphids. Insect Biochem. Mol. Biol. 105, 69–78. https://doi.org/10.1016/j.ibmb.2019.01.005.

Ross, P.D., and Subramanian, S. (1981). Thermodynamics of protein association reactions: forces contributing to stability. Biochemistry 20, 3096–3102. https://doi.org/10.1021/bi00514a017.

Saladin, B., Leslie, A.B., Wüest, R.O., Litsios, G., Conti, E., Salamin, N., and Zimmermann, N.E. (2017). Fossils matter: improved estimates of divergence times in Pinus reveal older diversification. BMC Evol. Biol. 17, 95. https://doi.org/10.1186/s12862-017-0941-z.

Stamatakis, A. (2014). RAxML version 8: a tool for phylogenetic analysis and post-analysis of large phylogenies. Bioinformatics 30, 1312–1313. https://doi.org/10.1093/bioinformatics/btu033.

Swarup, S., Williams, T.I., and Anholt, R.R.H. (2011). Functional dissection of Odorant binding protein genes in Drosophila melanogaster. Gene Brain Behav. 10, 648–657. https://doi.org/10.1111/j.1601-183x.2011.00704.x.

Turlings, T.C., and Erb, M. (2018). Tritrophic interactions mediated by herbivore-induced plant volatiles: mechanisms, ecological relevance, and application potential. Annu. Rev. Entomol. 63, 433–452. https://doi.org/10.1146/annurev-ento-020117-043507.

Urano, T. (2003). Preliminary release experiments in laboratory and outdoor cages of Dastarcus helophoroides (Fairmaire) (Coleoptera: Bothrideridae) for biological control of Monochamus alternatus Hope (Coleoptera: Cerambycidae). Bull. For. For. Prod. Res. Inst. 2, 255–262.

Vandermoten, S., Francis, F., Haubruge, E., and Leal, W.S. (2011). Conserved odorant-binding proteins from aphids and eavesdropping predators. PLoS One 6, e23608. https://doi.org/10.1371/journal.pone.0023608.

Vieira, F.G., and Rozas, J. (2011). Comparative genomics of the odorant-binding and chemosensory protein gene families across the Arthropoda: origin and evolutionary history of the chemosensory system. Genome Biol. Evol. 3, 476–490. https://doi.org/10.1093/gbe/evr033.

Vieira, F.G., Sánchez-Gracia, A., and Rozas, J. (2007). Comparative genomic analysis of the odorant-binding protein family in 12 Drosophila genomes: purifying selection and birth-and-death evolution. Genome Biol. 8, R235. https://doi.org/10.1186/gb-2007-8-11-r235.

Visser, J. (1988). Host-plant finding by insects: orientation, sensory input and search patterns. J. Insect Physiol. 34, 259–268. https://doi.org/10.1016/0022-1910(88)90056-x.

Vogt, R.G., and Riddiford, L.M. (1981). Pheromone binding and inactivation by moth antennae. Nature 293, 161–163. https://doi.org/10.1038/293161a0.

Wang, Q., Zhou, J.J., Liu, J.T., Huang, G.Z., Xu, W.Y., Zhang, Q., Chen, J.L., Zhang, Y.J., Li, X.C., and Gu, S.H. (2019). Integrative transcriptomic and genomic analysis of odorant binding proteins and chemosensory proteins in aphids. Insect Mol. Biol. 28, 1–22. https://doi.org/10.1111/imb.12513.

Wei, J.R., Yang, Z.Q., Hao, H.L., and Du, J.W. (2008). (R)-(+)-limonene, kairomone for Dastarcus helophoroides, a natural enemy of longhorned beetles. Agric. For. Entomol. 10, 323–330. https://doi.org/10.1111/j.1461-9563.2008.00384.x.

Wei, J.R., Yang, Z.Q., Poland, T.M., and Du, J.W. (2009). Parasitism and olfactory responses of Dastarcus helophoroides (Coleoptera: Bothrideridae) to different Cerambycid hosts. Biocontrol 54, 733–742. https://doi.org/10.1007/s10526-009-9224-y.

Xu, H., and Turlings, T.C.J. (2018). Plant volatiles as mate-finding cues for insects. Trends Plant Sci. 23, 100–111. https://doi.org/10.1016/j.tplants.2017.11.004.

Xu, P.X., Zwiebel, L.J., and Smith, D.P. (2003). Identification of a distinct family of genes encoding atypical odorant-binding proteins in the malaria vector mosquito, Anopheles gambiae. Insect Mol. Biol. 12, 549–560. https://doi.org/10.1046/j.1365-2583.2003.00440.x.

Xu, Y.L., He, P., Zhang, L., Fang, S.Q., Dong, S.L., Zhang, Y.J., and Li, F. (2009). Large-scale identification of odorant-binding proteins and chemosensory proteins from expressed sequence tags in insects. BMC Genom. 10, 632. https://doi.org/10.1186/1471-2164-10-632.

Yang, Z.H. (2007). Paml 4: phylogenetic analysis by maximum likelihood. Mol. Biol. Evol. 24, 1586–1591. https://doi.org/10.1093/molbev/msm088.

Yang, Z.H., and Nielsen, R. (2000). Estimating synonymous and nonsynonymous substitution rates under realistic evolutionary models. Mol. Biol. Evol. 17, 32–43. https://doi.org/10.1093/oxfordjournals.molbev.a026236.

Yang, Z.Q., Wang, X.Y., and Zhang, Y.N. (2014). Recent advances in biological control of important native and invasive forest pests in China. Biol. Control 68, 117–128. https://doi.org/10.1016/j.biocontrol.2013.06.010.

Zhang, J.Z., and Yang, J.R. (2015). Determinants of the rate of protein sequence evolution. Nat. Rev. Genet. 16, 409–420. https://doi.org/10.1038/nrg3950.

Zhang, S.Q., Che, L.H., Li, Y., Liang, D., Pang, H., Ślipiński, A., and Zhang, P. (2018). Evolutionary history of Coleoptera revealed by extensive sampling of genes and species. Nat. Commun. 9, 205. https://doi.org/10.1038/s41467-017-02644-4.

Zhou, J.J., Zhang, G.A., Huang, W.S., Birkett, M.A., Field, L.M., Pickett, J.A., and Pelosi, P. (2004). Revisiting the odorant-binding protein LUSH of Drosophila melanogaster: evidence for odour recognition and discrimination. FEBS Lett. 558, 23–26. https://doi.org/10.1016/s0014-5793(03)01521-7.

STAR★METHODS

KEY RESOURCES TABLE

REAGENT or RESOURCE	SOURCE	IDENTIFIER
Antibodies		
Rabbit polyclonal anti-MaltOBP24	This paper	N/A
Rabbit polyclonal anti-DhelOBP10	This paper	N/A
Rabbit polyclonal anti-β-Tubulin	Yeasen	Cat#30302ES20
Rabbit polyclonal anti-GAPDH	AtaGenix	Cat#ATPA00013Rb
Peroxidase-Conjugated Goat Anti-Rabbit IgG(H + L)	Yeasen	Cat#33101ES60
Bacterial and virus strains		
Transetta (DE3) Chemically Competent Cell	TransGen Biotech	Cat#CD801-02
Biological samples		
M. alternatus	Yichang, Hubei, PR China (110° 29 E; 30° 70 N)	N/A
D. helophoroides	Chinese Academy of Forestry	http://en.caf.ac.cn/
Chemicals, peptides, and recombinant proteins		
TRIzol reagent	Invitrogen	Cat#15596-018
Restriction Endonucleases EcoRI	New England Biolabs	Cat#R0101S
Restriction Endonucleases XhoI	New England Biolabs	Cat#R0146S
T4 DNA Ligase	New England Biolabs	Cat#M0202S
TEV Protease (His-tag)	Beyotime	Cat# P2307
RIPA Lysis Buffer	Beyotime	Cat#P0013D
Electrochemiluminescence (ECL)	Beyotime	Cat#P0018S
Isopropyl-beta D-thiogalactopyranoside (IPTG)	Sigma-Aldrich	Cat#I1284
Tris	BioFroxx	Cat#1115
N-Phenyl-1-naphthylamine (1-NPN)	Sigma-Aldrich	Cat#104043
(+)-fenchone	Sigma-Aldrich	Cat#46208
α-terpinolene	Sigma-Aldrich	Cat#43905
3-carene	Sigma-Aldrich	Cat#94415
R-(+)-limonene	Sigma-Aldrich	Cat#62118
S-(-)-limonene	Sigma-Aldrich	Cat#62128
(+)-limonene oxide	Sigma-Aldrich	Cat#218324
Camphene	Sigma-Aldrich	Cat#442505
Camphor	Sigma-Aldrich	Cat#21310
β-caryophyllene	Sigma-Aldrich	Cat#22075
(-)-caryophyllene oxide	Sigma-Aldrich	Cat#22076
(+)-α-longipinene	Sigma-Aldrich	Cat#62638
Myrcene	Sigma-Aldrich	Cat#64643
(+)-α-pinene	Sigma-Aldrich	Cat#80605
(+)-β-pinene	Sigma-Aldrich	Cat#80607
Critical commercial assays		
PrimeScript II 1st Strand cDNA Synthesis Kit	TaKaRa	Cat#6210A
BCA Protein Assay Kit	Beyotime	Cat#P0012S
T7 Ribo Max Express RNAi System	Promega	Cat#P1700

(Continued on next page)

Continued

REAGENT or RESOURCE	SOURCE	IDENTIFIER
Oligonucleotides		
Primers, see Table S4	This paper	N/A
Recombinant DNA		
Plasmid: pET-32b-MaltOBP24	This paper	N/A
Plasmid: pET-32b-DhelOBP10	This paper	N/A
Software and algorithms		
SignalP	DTU Health Tech	http://www.cbs.dtu.dk/services/SignalP/
MAFFT	EMBL-EBI	https://www.ebi.ac.uk/Tools/msa/mafft/
RAxML	(Kumar et al., 2018)	v8.2.10
Evolview-v2	(He et al., 2016)	https://evolgenius.info//evolview-v2/
ESPript 3.0	SBGrid	https://espript.ibcp.fr/ESPript/cgi-bin/ESPript.cgi
PAML 4.9	(Yang, 2007)	http://abacus.gene.ucl.ac.uk/software/paml.html
MEME Suite 5.4.1	(Bailey et al., 2015)	https://meme-suite.org/meme/tools/meme
MEGA X	(Kumar et al., 2018)	https://www.megasoftware.net/

RESOURCE AVAILABILITY

Lead contact

Further information and requests for resources and reagents should be directed to and will be fulfilled by the lead contact, Manqun Wang (mqwang@mail.hzau.edu.cn).

Materials availability

All plasmids and antibodies generated in this study are available from the lead contact without restriction.

Data and code availability

This study did not generate any unique datasets. All data generated during this study are either supplied in the figures and the supplemental information or will be shared by the lead contact upon request. This paper does not report original code.

Any additional information required to reanalyze the data reported in this paper is available from the lead contact upon request.

EXPERIMENTAL MODEL AND SUBJECT DETAILS

Newly emerged *M. alternatus* adults were collected from dead *P. massoniana* trees from Yichang, Hubei, PR China (110° 29 E; 30° 70 N). Fresh *P. massoniana* twigs were used to feed the adults which were reared in the plastic feeding boxes individually at 25°C. 10-day-old males and females were paired in a plastic bottle (30 cm diameter, 30 cm length).

D. helophoroides pupae and adults were provided by the Research Institute of Forest Ecology, Environment and Protection, Chinese Academy of Forestry. Laboratory colonies of *D. helophoroides* were initially been gathered from parasitized larvae and pupae of *M. alternatus*. *D. helophoroides* pupae and adults were reared at 25°C in ventilated plastic boxes. Adults were fed on an artificial diet (dried meat floss of *M. alternatus* larvae and pupae).

METHOD DETAILS

Y-tube olfactometer experiments

The binary choice assay of *M. alternatus* adults or *D. helophoroides* adults in different treated groups to chosen chemicals was performed in Y-tube olfactometers placed in a bandbox with a daylight LED lamp for illumination. For *M. alternatus*, the central tube was 40 cm long and the two branching arms were 30 cm long with the angle of 60° between them. For *D. helophoroides*, the central tube was 15 cm long

and the two branching arms were 12 cm long with the angle of 75° between them. A vial containing a 1 × 1 cm filter paper was connected to a branching arm. 10μL of chemical diluted 100 times with paraffin oil was added to the filter paper in one of the vials, while 10μL of paraffin oil was dropped into the other vial as a control. The air flow through each arm of the olfactometer was controlled to 300 mL/min and the filter paper in each vial was replaced every 10 min.

8 days adult insects were used for this test. Each insect was placed at the base of the central arm of the Y-tube and was allowed 5 min to make a choice between the odorant and the control. Its choice was recorded when it crawled to 1/2 of the branching arm. After observation of 5 individuals, the two arms were exchanged to avoid position effects. After observation of 10 individuals, the two arms were exchanged to avoid unidirectionality. At least sixty (30 females and 30 males) adult insects in each treated group were detected and were only tested once.

After ten trials, the Y-tube olfactometer equipment was cleaned with alcohol and dried by drying oven at 140 °C.

Phylogenetic analysis

Phylogenetic analysis was performed using amino acid sequences of 223 OBPs from ten species of eight superfamilies in Coleoptera, including *M. alternatus*, *D. helophoroides*, *H. axyridis*, *C. bowringi*, *C. formicarius*, *A. tumida*, *T. castaneum*, *R. dominica*, *H. oblita*, *N. vespilloides*. CSPs from *M. alternatus* and *D. helophoroides* were used as outgroups (Table S4). These amino acid sequences were obtained from NCBI (www.ncbi.nlm.nih.gov/) and their signal peptides were predicted by SignalP (http://www.cbs.dtu.dk/services/SignalP/). Sequences without signal peptides were aligned using the program MAFFT (https://www.ebi.ac.uk/Tools/msa/mafft/). A maximum-likelihood phylogenetic tree was constructed using RAxML (v8.2.10) (Stamatakis, 2014) with the Jones-Taylor-Thornton amino acid substitution model (JTT). The node support of tree branches was assessed by 1000 bootstrap replicates. Finally, the tree was viewed and edited with Evolview-v2 (https://evolgenius.info//evolview-v2/) (He et al., 2016).

The amino acid sequences (without signal peptides) of 234 OBPs from fourteen species of common herbivorous insects and enemies, including *M. alternatus*, *D. helophoroides* and *H. axyridis* from Coleoptera; *S. avenae*, *N. lugens*, *C. lividipennis* and *E. heros* from Hemiptera; *P. xylostella* and *D. punctatus* from Lepidoptera; *C. vestalis*, *T. dendrolimi* and *T. podisi* from Hymenoptera; *E. balteatus* from Diptera; *C. pallens* from Neuroptera, and CSPs from *M. alternatus* and *D. helophoroides* were used as outgroups were used to conducted a maximum likelihood phylogenetic tree with the same method above (Table S4) (Liu et al., 2020).

Amino acid sequence analysis and selection pressure analysis

Pairwise sequence alignments of each pair of OBPs from herbivores and enemies were performed using EMBOSS Needle (https://www.ebi.ac.uk/Tools/psa/emboss_needle/), which can provide the values of identity and similarity. ESPript 3.0 (https://espript.ibcp.fr/ESPript/cgi-bin/ESPript.cgi) was used to visualize the results of pairwise and multiple sequence alignments.

The ratio ω = dN/dS (where dN and dS are the nonsynonymous and synonymous substitution rates, respectively) was used to analyze the selective pressure acting on the Coleoptera OBPs of each clade (A-D) with a pair of homologous OBPs respectively from *M. alternatus* and *D. helophoroides*. Under strict neutrality, the expected ratio (ω) equals 1. ω > 1 and ω < 1 indicate positive selection and purifying selection, respectively. The OBP genes without complete sequence (RdomOBP8, AtumOBP6) were removed when performing calculation. The codon sequences in each clade were aligned using ClustalW procedure and MEGA X software was used to conduct maximum likelihood phylogenetic trees separately (Kumar et al., 2018). ω was calculated with the CodeML procedure from PAML 4.9 package with Run mode = 0: user tree, Model = 0: one-ratio. Further statistic tests were conducted by comparison of two pairs of site models with likelihood ratio test (LRT) and df = 2 was used. The first pair include M1a (neutral) and M2a (selection), with NSsites = 1, 2. The second pair include M7 (beta) and M8 (beta&ω), with NSsites = 7, 8 (Yang, 2007).

ω was also used to analyze the selective pressure acting on the paired OBPs respectively from herbivores and enemies. The codon sequences were aligned using ClustalW procedure. ω was calculated with the

CodeML procedure from PAML 4.9 package with Runmode = −2: pairwise (Goldman and Yang, 1994; Yang and Nielsen, 2000).

Evolutionary rate analysis

The evolutionary rate between MaltOBP24 and DhelOBP10, MaltOBP19 and DhelOBP22, MaltOBP16 and DhelOBP16, MaltOBP10 and DhelOBP13 is calculated with Zuckerkandl-Pauling-Kimura method: n_{aa} is the total number of amino acid sites in two polypeptide chains compared with each other (preferably excluding deletions and insertions), and d_{aa} is the number of sites in which they are different. K_{aa} means the number of substitutions per amino acid site over the evolutionary period that separated these two polypeptides. Assuming independence of substitution, we have K_{aa} = -ln(1-p_d), where p_d = d_{aa}/n_{aa} is the fraction of different sites. The rate of substitution per amino acid site per year is obtained from kaa = Kaa/(2T), where T is the number of years elapsed since divergence from a common ancestor. When different proteins from the same species pair are compared, p_d may be directly compared because T is the same for the proteins under consideration (Kimura, 1969; Nei and Kumar, 2000; Zhang and Yang, 2015).

Motif analysis

Motif analysis was conducted to check whether the OBPs from clade A which contained MaltOBP24 and DhelOBP10 have similar motif structures using MEME Suite 5.4.1 (https://meme-suite.org/meme/tools/meme) (Bailey et al., 2015). The parameters used for motif discovery were minimum width = 6, maximum width = 50, and the maximum number of motifs to find = 6.

Tissues collection

For the *MaltOBP24* and *DhelOBP10* genes cloning and tissue expression profiling, different tissues (antennas, heads without antennae, abdomens, wings, and legs) in different development stages (For *M. alternatus*: 2 days, 4 days, 6 days, 8 days, 10 days, 12 days, 14 days after emergence; For *D. helophoroides*: unmated adults, preoviposition duration adults, and oviposition peak duration adults) of male and female adults are collected separately. To detect the effect of RNAi on the expression of MaltOBP24 and DhelOBP10, antennae were collected on d 4 after each treatment (non-injection control, dsGFP injection and dsMaltOBP24 or dsDhelOBP10 injection). The tissue samples were stored in liquid nitrogen, nucleic acid samples and proteins stored at −80°C.

Total RNA extraction and cDNA synthesis

According to the manufacturer's protocol, total RNA was extracted from different tissues by TRIzol reagent (Invitrogen, Carlsbad, CA, USA). The purity and concentration of total RNA were assessed using an UV spectrophotometer (Eppendorf BioPhotometer Plus, Hamburg, Germany). For gene cloning and quantitative real-time PCR analysis, cDNA was synthesized from 1 μg of RNA using the PrimeScript II 1st Strand cDNA Synthesis Kit (TaKaRa Bio, Otsu, Japan) according to the manufacturer's instructions.

Quantitative real-time PCR (qRT-PCR)

The expression profiles of MaltOBP24 and DhelOBP10 in the antenna of different development stages and different adult tissues were analyzed using real-time RT-PCR. qRT-PCR was performed using the CFX96 Touch Real-Time PCR Detection System (Bio-Rad, California, USA) and Hieff qPCR SYBR Green Master Mix (Yeasen, Shanghai, China). β-Actin was used as an internal control in *M. alternatus* and RPS was used as an internal control in *D. helophoroides*. The primers (Table S5) were designed by Primer-BLAST (http://www.ncbi.nlm.nih.gov/tools/primer-blast/). The reaction was carried out in a 20 μL reaction system containing 10 μL Hieff qPCR SYBR Green Master Mix, 0.5 μL each primer(10 μM), 1 μL template cDNA, and 8 μL sterilized ultrapure H_2O. The PCR conditions were 5 min at 95°C, followed by 40 cycles of 10 s at 95°C, 30 s at 60°C, followed by 95°C for 15 s, 60°C for 1 min, 95°C for 15 s. The $2^{-\Delta\Delta Ct}$ method was used to calculate the relative mRNA expression levels.

Protein expression and purification

Gene specific primers (Table S5) with restriction sites (EcoRI and XhoI) were designed to clone cDNAs encoding MaltOBP24 and DhelOBP10. The forward primers contained His-tags. PCR were performed using 2×Hieff PCR Master Mix (Yeasen, Shanghai, China). The purified PCR products were subcloned into the bacterial expression vector pET-32b using EcoRI and XhoI restriction enzymes (New England Biolabs, Massachusetts, USA). The recombinant plasmids containing correct insert were then transformed into

Transetta (DE3) Chemically Competent Cell (TransGen, Beijing, China). Single positive clone verified by sequencing was inoculated in Luria-Bertani broth containing ampicillin with shaking at 220 rpm and at 37°C for large-scale culture. Protein expression was induced by adding IPTG (isopropyl-beta D-thiogalactopyranoside) to a final concentration of 1 mM when the culture reached an optical density of 0.6–0.8 at 600 nm. After incubating at 200 rpm for another 12 h at 16°C, the proteins were harvested by centrifugation (7000 rpm, 5 min) and lysed by sonication. The sodium dodecyl sulfate polyacrylamide gel electrophoresis (SDS-PAGE) analysis showed that MaltOBP24 and DhelOBP10 were present mainly in the soluble part.

The proteins were subsequently purified using Ni Sepharose 6 Fast Flow (GE Healthcare, Uppsala, Sweden). To remove the His-tags, TEV Protease (Beyotime, Shanghai, China) was used. The tag-free proteins were obtained in the eluted fraction after running the digested protein back through the Ni Sepharose 6 Fast Flow. SDS-PAGE monitored all purification steps. The purified proteins were dialyzed in Tris buffer (pH7.4 or pH5.0) for subsequent assays.

Fluorescence binding assays

Successfully expressed and purified recombinant MaltOBP24 and DhelOBP10 proteins without signal peptides were used in fluorescence binding assays and fluorescence-quenching spectra assays to explore binding properties with host plant volatiles (Campanacci et al., 2001).

The binding affinity of MaltOBP24 and DhelOBP10 for 14 common volatiles from forest (Table S6) was measured by fluorescence competitive binding assays on a RF-5301PC fluorescence spectrophotometer (Shimadzu, Kyoto, Japan). The fluorescent probe 1-NPN and ligands were diluted with spectrophotometric-grade methanol to a final concentration of 1 mM. The binding characterization of the fluorescent probe 1-NPN with MaltOBP24 and DhelOBP10 were analyzed first. The probe 1-NPN was excited at 337 nm and the scan range was between 350 and 600 nm. Purified recombinant proteins diluted to 2 M solutions with 30 mM Tris-HCl (pH7.4 or pH5.0) were titrated with the 1 mM 1-NPN solution to final concentrations ranging from 0 to 24 μM for DhelOBP10 and from 0 to 20 μM for MaltOBP24 to determine the dissociation constants (K_d) for 1-NPN. Aliquots of 1 mM competitor ligand were added to the solution containing both protein and 1-NPN at 2 μM to a final concentration ranging from 0 to 20μM. Dissociation constants of the competitors, Ki, were calculated according to the following equation: $Ki = [IC_{50}]/(1 + [1\text{-NPN}]/K_{1\text{-NPN}})$, where IC_{50} is the concentration of competitors halving the initial fluorescence level, [1-NPN] is the free concentration of 1-NPN, and $K_{1\text{-NPN}}$ is the dissociation constant of the 1-NPN/proteins binding reaction determined by Scatchard analysis. A smaller value of Ki indicates a stronger binding capacity in this assay.

Fluorescence-quenching spectra

The fluorescence-quenching assays of MaltOBP24 and DhelOBP10 were performed using an RF-5301 PC fluorescence spectrophotometer (Shimadzu, Kyoto, Japan). The excitation and emission were 15 and 10 nm for both MaltOBP24 and DhelOBP10. The excitation wavelength was 283 nm for MaltOBP24 and 289 nm for DhelOBP10. The scan range were between 300 and 500 nm. To measure the fluorescence quenching for different ligands, aliquots of 1 mM ligand solution was added to the 2 μM solution of MaltOBP24 or DhelOBP10 diluted by 30 mM Tris-HCl (pH7.4 or pH5.0) at the temperatures of 289 and 298 K. The temperature was controlled by an electronic thermostat water bath (9012, PolyScience, Niles, IL, USA).

The interaction between the fluorescent sample and the quencher can be divided into dynamic quenching and static quenching. Dynamic quenching is formed by collisions between the fluorophore and quencher, and static quenching results from binding between the fluorescent sample and the quencher (Lakowicz, 2008). The quenching mechanism of a reaction can be determined by the Stern-Volmer equation: $F_0/F = 1 + K_{sv}[Q] = 1 + K_q\tau_0[Q]$, where K_{sv} is the Stern-Volmer dynamic quenching constant; F_0 and F are the fluorescence intensity in the absence or presence of a quencher at concentration [Q], respectively; K_q is the quenching rate constant of the biomolecule; τ_0 is the average lifetime of the molecule without a quencher with a value of 10^{-8} s.

Decreasing value of K_{sv} as the temperature increases and far greater K_q value than the maximal bimolecular quenching constant of various kinds of quenchers for biological macromolecules (2.0×10^{10} (L mol^{-1} s^{-1}))

indicate that the quenching mechanism is static, because higher temperature leads to lower binding stability of protein/ligand complexes and lower K_{sv} values during static quenching but leads to faster diffusion in dynamic quenching and higher K_{sv} values.

As for static quenching, further analysis can be made by the double logarithm equation: $lg[(F_0-F)/F] = lgK_a + nlg[Q]$, where K_a is the apparent association constant, and n is the number of binding sites per protein. n and K_a at different temperatures in the binding interaction between the volatiles and MaltOBP24/DhelOBP10 were calculated based on the double logarithm equation. When the value of n is close to 1, the ligands and MaltOBP24/DhelOBP10 are binding at a ratio of 1:1. Thermodynamic equations were used to calculate thermodynamic data and to determine the binding force: $\Delta G = -RTlnK$ $\Delta H = (RT_1T_2ln(K_2/K_1))/(T_2-T_1)$ $\Delta S= (\Delta H-\Delta G)/T$. ΔG, ΔH, and ΔS are the free energy change, enthalpy change, and entropy change, respectively. $\Delta G < 0$ suggests that these binding interactions are spontaneous. In a slight temperature change, the enthalpy change can be regarded as a constant. Theoretically, $\Delta H < 0$ and $\Delta S > 0$ indicates the main acting force is an electrostatic force; $\Delta H < 0$ and $\Delta S < 0$ indicates the main acting force is van der Waals force or hydrogen bonding; $\Delta H > 0$ and $\Delta S > 0$ indicates the main force is hydrophobic interaction (Ross and Subramanian, 1981).

dsRNA synthesis

dsRNA targeting MaltOBP24, DhelOBP10, or GFP was synthesized using the primers with a T7 docking sequence at the 5' end (Table S5) and the T7 Ribo Max Express RNAi System (Promega, USA). After purification using Isopropanol, Sodium Acetate and 70% ethanol, the dsRNA was resuspended using nuclease-free DEPC-treated water. The quality and concentration of the resultant dsRNA product were analysed using a spectrophotometer at 260 nm and agarose gel electrophoresis.

Microinjection of dsRNA

4-day-old *M. alternatus* adults and *D. helophoroides* adults were chosen for RNAi. There were three treated groups for each kind of insect: non-injected, dsGFP-injected, and dsMaltOBP24-injected or dsDhelOBP10-injected. 1 μg dsGFP or dsMaltOBP24 was injected into the frons of the *M. alternatus* adults after CO_2 narcosis and 300 ng dsGFP or dsDhelOBP10 was injected into the frons of the *D. helophoroides* adults immediately using a microinjector (World Precision Instruments Inc., Sarasota, FL, USA). After 4days of injection, samples were taken to check the effects of RNAi on the transcription level of the MaltOBP24 gene and the DhelOBP10 gene by qRT-PCR and on the protein level of by western blot. And the behavioral responses of different treatments were detected by the Y-tube olfactometer.

Western blot analysis

Antennae from *M. alternatus* and *D. helophoroides* in different treatments (non-injected, dsGFP-injected, and dsMaltOBP24-injected or dsDhelOBP10-injected) were homogenized in RIPA Lysis Buffer (Beyotime) to obtain total proteins. Protein concentrations were determined using the BCA Protein Assay Kit (Beyotime). 20 μg of the samples were denatured at 100 °C for 5 min in 4X SDS-PAGE loading buffer, separated by 15% SDS-PAGE gels and transferred to 0.45 μm PVDF membranes (Millipore, USA). After being blocked for 2 h at room temperature, the membranes were washed and incubated with specific primary antibodies diluted in 5% milk/PBST at 1:1500. The primary antibodies used in this study were as follows: Rabbit anti-MaltOBP24 antibody, Rabbit anti-DhelOBP10 antibody, Rabbit β-Tubulin Antibody (Yeasen), and Rabbit GAPDH Antibody (AtaGenix). Peroxidase-Conjugated Goat Anti-Rabbit IgG (H + L) (Yeasen) diluted in 5% milk/PBST at 1:4000 was used as the secondary antibody. Electrochemiluminescence (ECL) (Beyotime) and the chemiluminescence imaging system with a charge-coupled device (CCD) camera (Bio-Rad) was used for target protein detection.

QUANTIFICATION AND STATISTICAL ANALYSIS

Data are presented as the mean $\pm$ SEM. Statistical analysis was performed using one-way analysis of variance (ANOVA) or Chi-square test carried out by IBM SPSS Statistics 26.0. Post-hoc tests were performed using the Turkey method, and $p < 0.05$ was accepted as significant (shown by different letters); *, $p < 0.05$, **, $p < 0.01$.